Kaunas University of Technology

Faculty of Mathematics and Natural Sciences

Modeling of Heterogeneous Catalysis Processes on the Surface of Nanostructured Catalysts

Master's Final Degree Project

Emilija Ragėnaitė

Project author

Prof. habil. dr. Arvaidas Galdikas

Supervisor

Kaunas, 2022

Kaunas University of Technology

Faculty of Mathematics and Natural Sciences

Modeling of Heterogeneous Catalysis Processes on the Surface of Nanostructured Catalysts

Master's Final Degree Project

Materials Physics (6213CX001)

Emilija Ragėnaitė

Project author

Prof. habil. dr. Arvaidas Galdikas

Supervisor

Dr. Benas Gabrielis Urbonavičius

Reviewer

Kaunas, 2022

Kaunas University of Technology

Faculty of Mathematics and Natural Sciences

Emilija Ragėnaitė

Modeling of Heterogeneous Catalysis Processes on the Surface of Nanostructured Catalysts

Declaration of Academic Integrity

I confirm the following:

1. I have prepared the final degree project independently and honestly without any violations of the copyrights or other rights of others, following the provisions of the Law on Copyrights and Related Rights of the Republic of Lithuania, the Regulations on the Management and Transfer of Intellectual Property of Kaunas University of Technology (hereinafter – University) and the ethical requirements stipulated by the Code of Academic Ethics of the University;

2. All the data and research results provided in the final degree project are correct and obtained legally; none of the parts of this project are plagiarised from any printed or electronic sources; all the quotations and references provided in the text of the final degree project are indicated in the list of references;

3. I have not paid anyone any monetary funds for the final degree project or the parts thereof unless required by the law;

4. I understand that in the case of any discovery of the fact of dishonesty or violation of any rights of others, the academic penalties will be imposed on me under the procedure applied at the University; I will be expelled from the University and my final degree project can be submitted to the Office of the Ombudsperson for Academic Ethics and Procedures in the examination of a possible violation of academic ethics.

Emilija Ragėnaitė

Confirmed electronically

Ragėnaitė, Emilija. Modeling of Heterogeneous Catalysis Processes on the Surface of Nanostructured Catalysts. Master's Final Degree Project / supervisor prof. habil. dr. Arvaidas Galdikas; Faculty of Mathematics and Natural Sciences, Kaunas University of Technology.

Study field and area (study field group): Physics, Physical sciences

Keywords: Kinetic modeling, hydrogen, isotopic exchange, partial pressure, surface diffusion.

Kaunas, 2022. 53 pages.

Summary

A kinetic model for modeling H_2/D_2 isotopic exchange has been developed to characterize interactions between hydrogen species and ruthenium-based catalysts, referencing experimental results for such interactions found in literature. Processes, described by kinetic equations, and included in this kinetic model are adsorption on ruthenium sites, isotopic equilibration reaction on noble metal, desorption from the metal to the gas phase, and surface diffusion from the metal nanocluster to the support, as well as from the support to the cluster. The curves obtained by using the kinetic model computer code showed good agreement with the experimental data, therefore, the calculations have been extended beyond repeating the experiment – to analyze the influence of different parameters on the catalytic processes. Volume of the reactor, surface area of the noble metal in the catalyst, metal dispersion, mass, and mass fraction in the catalyst were separately analyzed in terms of their effect on the partial pressure. The reaction rate, that fits the experimental results, was found, as well as the influence of the reaction rate on the partial pressures has been analyzed. Surface diffusion was included in the kinetic model to show the effect it has on the surface concentration values of hydrogen and deuterium, not only on the metal sites, but also on the support.

Ragėnaitė, Emilija. Vandenilio izotopų heterogeninės katalizės procesų modeliavimas nanostruktūrizuotų katalizatorių paviršiuose. Magistro studijų baigiamasis projektas / vadovas prof. habil. dr. Arvaidas Galdikas; Kauno technologijos universitetas, Matematikos ir gamtos mokslų fakultetas.

Studijų kryptis ir sritis (studijų krypčių grupė): Fizika, Fiziniai mokslai

Reikšminiai žodžiai: Kinetinis modeliavimas, vandenilis, izotopų mainai, dalinis slėgis, paviršinė difuzija.

Kaunas, 2022. 53. p.

Santrauka

Sukurtas H_2/D_2 izotopų mainų ant katalizatorių paviršių kinetinis modelis, skirtas apibūdinti šių vandenilio rūšių ir rutenio katalizatorių sąveiką, remiantis literatūroje rastais eksperimentiniais tokios sąveikos rezultatais. Procesai, aprašyti kinetinėmis lygtimis ir įtraukti į šį kinetinį modelį, yra adsorbcija rutenio salelėse, izotopų pusiausvyros reakcija ant tauriojo metalo, desorbcija nuo metalo į dujų fazę ir paviršiaus difuzija nuo metalo nanoklasterio į atramą, taip pat nuo atramos link klasterio. Eksperimentiniai ir teoriniai rezultatai buvo suderinti pagal dalinio slėgio vertes laikui bėgant. Kreivės, gautos naudojant kinetinio modelio kompiuterinį kodą, gerai sutapo su eksperimentiniais duomenimis, todėl skaičiavimai buvo naudojami ne tik eksperimento atkartojimui, bet ir skirtingų parametrų įtakos kataliziniams procesams analizei. Atskirai buvo analizuojamas reaktoriaus tūris, tauriojo metalo paviršiaus plotas katalizatoriuje, metalo dispersija, masė ir masės dalis katalizatoriuje, atsižvelgiant į jų poveikį daliniam slėgiui. Nustatytas reakcijos greitis, atitinkantis eksperimento rezultatus, bei išanalizuota reakcijos greičio įtaka daliniams slėgiams. Paviršiaus difuzija buvo įtraukta į kinetinį modelį, siekiant parodyti jos poveikį vandenilio ir deuterio paviršinėms koncentracijoms ne tik metalo salalėse, bet ir ant atramos.

Table of contents

List of figures

List of tables

Introduction

Catalysts are used in a myriad of industries, beginning with the use in the automotive industry, ending with agricultural applications. Heterogeneous catalysis is a kind of catalysis that occurs between reactants and a catalyst that are of different states of matter, in this case, the solid catalyst, and gas reactants. This process consists of several sub-processes that are important when creating a kinetic model: adsorption, desorption, chemical reactions, and surface diffusion. Isotopic exchange is a tool that experimenters use to characterize interactions between the catalyst, and the chosen isotopes. In our work the isotopes are hydrogen and deuterium. We are building a kinetic model that will bring the reality and the simulation together to create a tool that can be utilized to manipulate parameters of the process on a computer and see theoretical results that sufficiently precisely represent the effect these parameter changes would have in real life.

The goal of this work. To develop a kinetic model for heterogeneous catalysis processes of hydrogen isotopes on the surface of nanostructured ruthenium-based catalysts and apply the model to analyze the influence of process parameters.

Tasks:

1. To analyze the experiment that is referenced in this work. Find the initial parameter values for the process, as well as parameters that define the ruthenium-based catalyst. Find which processes occur on the surface of the catalyst during the experiment.

2. Describe the processes that occur on the catalyst in the form of kinetic equations. Express the equations in the form that is suitable for "MATLAB" software. Include the parameters that were used in the experiment that is being referenced to be able to achieve the best fit of experimental and theoretical curves. Determine the reaction rate.

3. To tweak the parameters in a way that will allow to analyze their influence on the system. Analyze the influence of reactors volume, surface area of the noble metal, dispersion, mass, and mass fraction of metal.

4. Provide information about the surface concentrations of hydrogen and deuterium on the metal site, as well as on the support, when surface diffusion occurs on the surface of the catalyst.

5. Evaluate the differences between the experimental conditions. The first, that is performed using an equimolar mixture of H_2/D_2 initially, and the second, where only D_2 is introduced into the reaction chamber in the beginning.

1. Literature review

1.1. Heterogeneous Catalysis

Catalysts are fascinating substances that are tremendously useful in the food [1], medical [2], textile [3], automotive [4], and other industries. Their usefulness comes from their ability to accelerate chemical reactions. A relatively small amount of an appropriate catalyst will promote the desired reaction. The catalytic material is not affected, nor consumed during the chemical reaction, it only participates as a helping platform for the reaction to occur. A catalyst is a guide of sorts for the reaction to take the more energetically favorable path.

The working mechanism of a catalyst can be described as cyclical. First, the reactants adsorb on the surface of a catalyst and the bond between the reactants and the catalyst is formed. Next, the adsorbed reactants interact with each other to form the reaction product. The product can then desorb from the catalyst. As the reaction product desorbs from the catalyst, it is left open for other reactants to adsorb. When the catalyst is recovered by desorption of the product, the cycle continues without any damage done to the catalyst. However, the last statement is more correct theoretically than practically. There are certain circumstances under which the catalyst could be damaged and become less effective over time [5].

Heterogeneous catalysis is emphasized in this work, this type of catalysis is present when the reactants and the catalyst are of different phases, most commonly a solid catalyst, such as ruthenium, and gas or liquid reactants, such as nitrogen and hydrogen. Ruthenium, nitrogen, and hydrogen are the examples of choice because they are related to catalytic ammonia synthesis which is a great example of heterogeneous catalysis. Ammonia, its synthesis, and catalysts used in the synthesis process will be reviewed in this section.

1.1.1. Ammonia. Past, Current and Future Applications and Synthesis.

Ammonia synthesis is the backbone of heterogenous catalysis. This century old process of producing ammonia using catalysts serves as a textbook example of heterogenous catalysis, therefore, it is meaningful to have a basic understanding of ammonia as a compound, its synthesis, current and future applications of ammonia, and catalyst used in its production.

Anhydrous ammonia is a toxic, flammable, colorless gas. It has a distinct, suffocating odor. Dissolving ammonia in water creates liquid ammonia which turns into a gas on exposure with air. Ammonia occurs naturally or is synthetically produced. One nitrogen and three hydrogen atoms covalently bond to form ammonia [6].

Ammonia has a wide range of applications, one of the most important applications is related to the food we consume. Grains are a food source that many people heavily rely on all around the world, therefore, the demand for grains, as well as effective means to produce it, is high. Fertilizers are a big part of the solution when it comes to meeting these demands. There are many kinds of chemical fertilizers, based on phosphorus, potassium, however, the most widely used fertilizers are nitrogen-based. Nitrogenous fertilizers are derived from ammonia, though ammonia can also be directly applied into the soil. The function of biological molecules in plants, animals, and humans depends on nitrogen which makes it not only an excellent fertilizer but also an important component in medicines [7].

The fertilizer industry is the primary user of synthetic ammonia, nonetheless, ammonia is not limited to agricultural applications. It is used to produce nitrates, sulfates, phosphates, textiles, amides, amines, resins, plastics, cyanide, nitric acid, ammonium salts, dyes, and explosives. Ammonia can also be used to transport hydrogen. Furthermore, it does surprisingly well as an industrial refrigerant.

Aside from industrial applications, ammonia is also commonly used for more personal purposes, such as maintaining the living space, it can be found in air fresheners, cleaners, stain removers, and can even be used to purify water [8].

While ammonia has been used for over a century, the researchers maintain their interest in this compound. As the world changes, environmental regulations become stricter, the energetically demanding process of producing ammonia requires adjustments. Researchers working on this issue classify ammonia production into categories of brown, blue, and green ammonia, the method of production is the key difference in this classification.

Brown ammonia is produced using fossil fuels, such as natural gas and coal, as raw materials to produce hydrogen used in the ammonia synthesis process. The hydrogen is obtained by the steam reforming process of methane using an iron-based catalyst. Brown ammonia process is the standard for obtaining ammonia and is based on the Haber-Bosch process. With hydrogen obtained from fossil fuels, and nitrogen obtained from the air by a separation unit process, a catalytic reaction of the hydrogen and nitrogen takes place and produces ammonia. Nitrogen is obtained from the air by the process called secondary reforming. During this process the synthesis gas from the primary reforming process is combined with the air in the secondary reforming reactor at an elevated temperature of around 1000°C and pressure of around 30 bars. This classic process is reliable; however, it requires high energy consumption, especially during the hydrogen production step [9].

Blue ammonia production method focuses on reducing the carbon dioxide emissions by introducing a decarbonization process. Green ammonia production relates to zero carbon dioxide emissions, it employs renewable energy sources such as wind, water, and solar energy. If hydrogen is obtained by electrolysis of water, no carbon compounds will be used in the process at all. Introducing a carbon dioxide removal unit to the existing Haber-Bosch process can heavily reduce the emissions, therefore, it is meaningful to use for blue and green ammonia production processes. The application of certain systems has been relatively successful, for example liquid electrolyte-based systems, molten salt-based electrolyte systems, composite membrane-based systems, and polymer membrane-based systems. Unfortunately, the demand for ammonia far exceeds the production capabilities of what these methods and systems can offer today. To improve the ammonia synthesis production process, to make it more efficient while reducing energy consumption, researchers are exploring catalysts. Science often mimics the nature, considering that ammonia has been naturally produced at room temperature and atmospheric pressure by bacteria that contain nitrogenase (enzyme catalyst), possibly, the synthetic green ammonia process could be further developed by examining biological examples of ammonia synthesis [10].

Not only the ammonia synthesis process is on the way to becoming more sustainable with all the new promising findings and ever-growing knowledge, but researchers are also exploring new potential applications, such as using ammonia as fuel.

Currently hydrocarbon fuels are predominantly used for energy generation, however, using them results in emissions that contain pollutants that are harmful to the environment and human health. An

alternative carbon-free fuel is ammonia. It has advantages over hydrogen fuels, for example, higher volumetric energy density, cheaper storage, and lower costs of transportation. However, using ammonia as a fuel results in high NO_x emissions. This problem prevents it from being used on a large scale. Since ammonia has been produced for over a century, the process is well-known and stable, therefore, it would require quite minimal investments to replace hydrocarbon fuels by ammonia. It is predicted that ammonia will become the main marine fuel in the future [9, 11].

In many scenarios, understanding the past is helpful in perfecting the future. The thought patterns of pioneers in the field of ammonia synthesis are reflected in their theoretical knowledge and practical application, therefore, old methods of obtaining ammonia are briefly reviewed below.

The first ways to obtain ammonia back in the 19th century were either to recover it from coal, or to obtain it from natural saltpeter. With time the demand for ammonia, especially as a fertilizer, grew and new synthesis methods of obtaining nitrogen from the air were introduced, namely the electric arc process, calcium cyanamide process, and catalytic ammonia synthesis.

The electric arc method is based on a reaction between nitrogen and oxygen at high temperatures under electric arc, such reaction produces nitric oxide which oxidizes in the air (which has oxygen) and turns into nitrogen dioxide, then adsorption in water allows the formation of nitric acid. This method is limited due to its very high energy consumption.

The cyanamide process is based on a reaction between calcium carbide CaC_2 and nitrogen, forming calcium cyanamide:

$$CaC_2 + N_2 \rightarrow Ca(CN)_2 \quad (1)$$

This process produces the calcium cyanamide which can be used as a raw material to produce organic compounds containing nitrogen and cyanides. This process is less energetically demanding than the electric arc method.

Increasing demand for nitrogenous fertilizers meant that a way to produce enough ammonia was necessary, none of the methods mentioned above were sufficient. The method of catalytic ammonia synthesis solved the riddle and quickly became an inseparable part of agriculture.

During the 20th century catalytic ammonia synthesis was very significant in the development of the chemical industry and inspired the scientific community to research and improve catalysts used for this purpose, as well as extend the research to other areas of catalysis such as characterization techniques and theoretical analysis of kinetics.

Ammonia synthesis process serves as an ideal model chemical reaction because it does not have a side reaction and its selectivity is 100%. This process fundamentally describes heterogenous catalysis, hence earning the title of a “textbook catalyst”. Understanding catalytic ammonia synthesis allowed further concepts of catalysis to be developed.

As mentioned earlier, the CO_2 emissions play an important role in the industrial processes, it has become more important than ever to find ways to make these processes as efficient as possible. This encourages new research in the field. Effective ways to reduce the energy consumption in chemical production are to innovate the process and find the most suitable catalysts. Better catalysts could increase the efficiency of production and allow the ammonia synthesis process to be carried out at

lower pressure, which would reduce the energy consumption. Progress in the catalytic ammonia synthesis field resulted in significant pressure reduction of the process: in the early days the process pressure range was 20 – 100 MPa, nowadays significantly lower pressure values of 8 – 10 MPa are possible. Not only is it important to research existing catalysts and develop new ones but also to improve the purification technology of synthesis gas; it is significant due to the risk of catalysts getting poisoned by the impurities in the synthesis gas. Energy consumption is also impacted by catalysts. Modern ammonia plants consume about $30 \cdot 10^9$ J per ton of ammonia with the theoretical value of this process being $22 \cdot 10^9$ J, this difference could be reduced by innovating the catalysts and making the process more efficient. Current technology allows 20% – 30% conversion rate from hydrogen and nitrogen to ammonia in one pass before being recycled. To increase this rate per pass catalysts with better activities at lower temperatures and pressures are needed [7].

1.1.2. Ammonia synthesis catalysts

Catalysts have been used for ammonia synthesis ever since 1909 when the first suitable catalyst was discovered and applied for this purpose. Not only was this a historical moment in the field of ammonia synthesis but it also served as a basis for the research and development of fundamental theories and concepts of heterogenous catalysis.

For about a century it was believed that fused iron catalysts with Fe_3O_4 precursor were superior in terms of activity. This belief limited the research related to magnetite-based catalysts; they were seen as not needing improvements for a very long time. These catalysts are still commonly used in the ammonia synthesis industry, even though their design is remarkably similar to the one developed roughly a century ago. Better iron containing catalysts have since been discovered, such as $Fe_{1-x}O$ based catalysts that are commonly used in ammonia synthesis process. These catalysts have higher activity than the best magnetite-based catalysts.

Inevitably, the curiosity, effort, and hard work of researchers resulted in discoveries of other catalysts. In the search of an excellent industrial catalyst Haber back in 1909 found osmium to be a promising catalyst as it had great activity in ammonia synthesis. Using nitrogen and hydrogen as the raw materials and an osmium catalyst he was able to obtain 90 g of ammonia at 600 °C and 175 atm pressure. Unfortunately, osmium is too rare and expensive to be used industrially. Another example of a catalyst with great activity but uncommon application is uranium, that has to do with the fact that traces of water or oxygen can easily poison this catalyst.

With fused iron catalysts being considered optimal, the interest of the researchers shifted towards non-iron based catalysts, these circumstances were favorable for the ruthenium catalysts to be discovered. Ruthenium catalysts on high surface area graphite support have been used for ammonia synthesis since 1992 [7].

Ruthenium-based catalysts can be used under lower synthesis pressure and temperature, they are less sensitive to NH_3 concentration in gas phase than magnetite-based catalysts and have a higher conversion rate. $Ru_3(CO)_{12}$ is commonly used to prepare ruthenium catalysts. Chlorine- and sulfur-containing compounds have a negative impact on the activity of the catalysts, these are severe poisons for NH_3 synthesis, so it is important to use a Ru precursor that is free of these compounds, such as the already mentioned $Ru_3(CO)_{12}$, and $Ru(NO)(NO_3)_3$.

Ruthenium catalysts can be prepared on various supports, such as MgO and Al_2O_3. In this study [12] Muhler et al. prepared ruthenium-based catalysts on MgO and Al_2O_3 supports, Cs and K promoted, and non-promoted catalysts were prepared and analyzed. The study suggests that Al_2O_3 support with a higher surface area was more stable than MgO with the lower surface area. Using MgO as a support for both Cs-Ru, and Ru catalysts resulted in better catalytic activity than using Al_2O_3 as a support. The version of catalyst prepared with the Cs promoter also did better in terms of catalytic activity. Cs-Ru/MgO catalyst with the smallest metal surface area, smallest dispersion and biggest particle size was the most catalytically active of the four catalysts investigated. The kinetics of the interaction between N_2 and Ru were analyzed and showed that Cs promoter enhances the rate of dissociative chemisorption and the rate of recombinative desorption. Cs has been found to be a better promoter than K. Cs promotion is less efficient on Al_2O_3 support, than MgO. CsOH interacts more with the acidic Al_2O_3 support, and not with the metal Ru particles, which is the opposite when a basic MgO support is used.

Carbon supports degrade during the ammonia synthesis due to methanation in a hydrogen-containing medium. Methane formation is undesirable during the ammonia synthesis process, however, carbon materials with disordered structures (high number of defects) and a large surface area are prone to this effect. An example of methanation is the conventional ammonia synthesis process on iron catalyst with a carbon support at 500°C and P = 30 MPa.

The mechanism of methanation on ruthenium catalysts is explained by the authors [13] as dissociative activation of hydrogen on ruthenium and the migration or spillover of hydrogen atoms from the ruthenium onto the surface of the support. Authors conclude that most of the hydrogen migrates to the boundary of ruthenium particles so the carbon that is in contact with ruthenium experiences methanation first which causes sintering of neighboring ruthenium particles. These effects lead to the catalyst particle dispersion reduction and catalytic activity declining. The use of alkali (e.g., Cs, K) and alkali-earth (e.g., Ba) promoters can prevent the interaction of the support and the hydrogen by blocking the surface of the carbon support which protects the catalyst from the undesirable effects mentioned above. Another protective measure is the graphitization of carbon supports at temperatures up to 2000°C.

Chen et al. [14] investigated strontium niobates as potential supports for ruthenium catalysts in ammonia synthesis. $Sr_2Nb_2O_7$ support of crystalline phase and surface area of 87 m2/g performed as the best support for ruthenium catalyst out of ones investigated in their work. Cs and Ba promoters performed really well at enhancing the activity of this support. Authors of this work name methanation as a problematic phenomenon in ammonia synthesis on ruthenium catalyst that use carbon supports, this effect has been explained in more detail above. Methanation inhibition is a serious problem that can reduce the lifetime of a catalyst, making finding of Chen et al. very meaningful because an effective strontium niobate support could potentially replace a carbon support in the future. Authors conclude that barium and cesium promoted ruthenium catalyst with Sr2Nb2O7 support show superior activity for ammonia synthesis compared to cesium promoted ruthenium on MgO support (Cs-Ru/MgO catalyst is mentioned as superior in the work of Muhler et al.). These findings are very promising because MgO was considered to be one of the most active oxide supports currently used for ammonia synthesis catalysts.

One of the most significant achievements in ammonia synthesis is the application of alkali metal-promoted ruthenium catalyst on a graphite support with a high surface area. Ruthenium catalysts on

carbon supports are very unstable. Ruthenium is very catalytically active in the process of hydrogenation [15] of carbon, causing major problems in these catalysts. Methanation is often considered to be the primary reason for the deactivation of Ru/C catalysts. Graphitization of carbon is a commonly used strategy to reduce the methanation effect on Ru/C catalysts in a hydrogen-containing environment. Lin et al. studied the deactivation of a potassium-promoted ruthenium catalyst with a carbon support. They found that the process of carbon methanation is not necessarily the main or the only cause of the loss of activity in ruthenium catalysts with carbon supports. The formation of carbon monoxide due to the oxidation of carbon at high temperatures is related to the activity and stability of such catalysts. The formation of CO and CO_2, which is inevitable at temperatures higher than 500 °C if K-Ru/C catalyst is used, increases the loss of carbon in the support, this leads to the negative effect of sintering of metal ruthenium particles and decreases the rate of ammonia synthesis [16].

Kowalczyk et al. [17] analyzed the effect that potassium and barium promoters have on the stability of ruthenium catalysts with a carbon support when they are used for ammonia synthesis. They have found that potassium could increase the reaction rate of methanation. Barium, on the other hand, slows this reaction, working as an inhibitor of methane formation reaction, slowing it eight times compared to Ru/C catalyst without a promoter. Therefore, it also showed higher activity in ammonia synthesis than potassium-promoted catalyst, and ever surpassed the activity of one of the most used catalysts in the industry – fused-iron catalyst.

This group performed experiments on ruthenium catalysts on carbon with potassium and barium at an elevated temperature of 793 K for 24 h and found that it affects dispersion of ruthenium particles. A sample with K promoter showed that dispersion decreased three times, and the same amount of time decreased the ammonia synthesis activity. The overheating had only a very slight effect on the dispersion and activity for the sample with barium.

Rossetti et al. [18] showed that barium, cesium, and potassium promoters affect the temperature at which methanation starts. In fact, this group has prepared a carbon-supported ruthenium catalyst promoted not by one the mentioned promoters, but all of them, simultaneously. This mixture of promoters is showing great activity. Thermal and methanation resistance is the contribution of barium, while cesium inhibits metal sintering, and potassium adds to the activity. Atomic ratios of the promoter divided by ruthenium, that result in the most active and resistant to high temperatures catalyst, are 0.6, 1, and 3.5 for barium, cesium, and potassium, respectively. Researchers conclude that ruthenium-based catalysts on carbon supports benefit from the use of promoters, however, using a too much can result in the blocking of the active site of Ru, which might not decrease the efficiency of the catalyst, but will not allow the promoter to be used to its full potential – sometimes less is more.

Huazhang Liu [19] has reviewed ammonia synthesis catalysts over the last hundred years. Liu's review includes a comparison of ruthenium-based, and iron-based catalysts in terms of cost and abundance. Ruthenium is much more costly and scarce than iron [20]. Therefore, even if ruthenium catalysts have great activity, there are challenges that limit the use of it, namely, strong H_2 inhibition and methanation that results in decrease of the lifetime of the catalyst. Only 16 ammonia plants used ruthenium-based catalysts from 1992 to 2010, according to the author. This shows that theoretical work is of high importance now, as well as experimental work, only further research can result in the eventual industrial usage of these catalysts.

Wang et al. [21] performed the ammonia synthesis reaction over a ruthenium catalyst that uses a perovskite support $BaTiO_3$ and found that this type of a catalyst is highly active for this process. They attribute the success of this catalyst to the support being strongly basic and its combination with ruthenium. It is achieved by using an elevated temperature when reducing the catalyst. Strong interactions between the support and the metal allow the electrons to flow from the support to the surface of metal, which weakens the triple bond between nitrogen atoms, therefore, allowing N_2 to dissociate easier. Creating the conditions that encourage dissociation leads to enhanced activity, Wang's group concludes.

Cobalt-based catalysts are also used for ammonia synthesis. Karolewska et al. [22] studied the role ceria plays in these catalysts. They found that ceria works as a structural promoter that inhibits the sintering process of cobalt under the conditions of ammonia synthesis reaction. Sintering lowers the effectiveness of the catalyst as it reduces dispersion of the catalytic material. The impact of ceria is also meaningful in catalysts that use barium as a promoter, it shows higher activity for ammonia synthesis than barium alone, especially when the amount of ceria is between 10 wt% and 13 wt%. This type of cobalt catalyst with barium and ceria promotion is also heat-resistant and can withstand a harsh treatment of 600 °C for 160 hours with resulting in slightly reduced activity.

Ru/Al_2O_3 catalysts, that were prepared using wet impregnation, colloidal method, and microemulsion, were analyzed by Fernández et al. [23] to study the effect of different average ruthenium particle sizes on ammonia synthesis process. It was found that good activity is achieved when using quite large particles, which is an unusual claim, however, it is the average size of the particles, the size distribution was broad, which resulted in an interesting effect where small and large nanoparticles cooperate. Small particles contain highly active sites, and big particles promote the reaction on the small ones. Large particles contribute to the increased transfer of hydrogen atoms as well as their activation, which promotes hydrogenation of nitrogen atoms that are strongly adsorbed, which releases the active sites, under mild conditions that is. This appears to be the case of a catalyst that adsorbs an atom strongly enough that it could be damaging to the process, because if the active sites are taken up, the process cannot go forward. Having a broad distribution of ruthenium particles can help relieve this symptom. This is because the large particles act as sites for hydrogen to adsorb on, that hydrogen can experience spillover from those large sites to the support and travel to the small particles in reverse spillover process. Additional hydrogen, that reaches the small particle this way, can hydrogenate the strongly adsorbed nitrogen, and help it desorb, so the active site is free again for the desirable reaction of ammonia synthesis to occur on. This results in increased catalytic activity.

Further research on ruthenium is necessary and meaningful in the process of widening the application of ruthenium-based catalysts industrially.

1.2. Isotopic exchange and modeling

Molecular dynamics is described [24] as a simulation method that investigates atoms and their location in space. The motion of these atoms is described by dynamic equations, based on classical Newtonian dynamics. Solving these equations by using numerical methods allows for simulating the motion of atoms or molecules.

Molecular dynamics simulations can be used to analyze hydrogen isotopic exchange. O. Lindblom et al. [25] apply this simulation method for analyzing the exchange of tritium (T) and protium (H) in tungsten vacancies. The goal of their simulation is to understand the underlying mechanisms of such

exchange of hydrogen isotopes, as it is important for nuclear fusion applications. Tritium can get trapped in the walls of the reactor, which may result in safety issues. Hydrogen can replace the tritium that is in a vacancy (which is in a wall of a reactor) by the isotopic exchange process. This group showed that vacancies resulting from irradiation exhibit isotopic exchange at low temperatures. Simulating this process at 500 K, it took only 100 ns for tritium to be completely exchanged with protium, and 3000 ns for 400 K. Interestingly, if the same temperatures are used, however, hydrogen is not introduced into the system, it takes significantly longer for tritium to be released from the vacancies, meaning that isotopic exchange results in better mobility of tritium than elevated temperatures alone.

Detritiation process by isotopic exchange was also analyzed by Lu et al. [26], their work is an example of such exchange of gas and liquid phase hydrogen-containing compounds. This allows to analyze the impact of hydrophobicity of the catalyst for the catalytic activity. Not only that, liquid phase catalytic exchange also requires hydrophobic catalysts to inhibit the process of liquid water "coating" the catalyst with a carbon or metal oxide support, because it would make the catalyst ineffective by restricting the access of hydrogen and water vapor to the catalyst. Considering this "coating" effect is important for Lu's groups research as they are looking to create a catalyst that is suitable for detritiation by isotopic exchange regarding nuclear reactor waste containing radioactive tritium.

Kinetic modeling, that is based on kinetic equations, is a macroscopic method. It differs from molecular dynamics in a way that the motion of individual particles is not considered in kinetic modeling, instead, the flux of these particles is considered [27]. Not having to calculate the movement of each particle makes it less resource-consuming, therefore, even a personal computer can be used for kinetic modeling. Simple molecular dynamics simulations can also be performed this way; however, additional resources are needed for more complicated projects, therefore, tools such as LAMMPS Molecular Dynamics Simulator is used.

Not only molecular dynamics simulations, but also kinetic simulations are used to analyze isotopic exchange. One of the scenarios is the exchange of hydrogen isotopes between water and methane (CH_4), which has been researched by Turner et al. [28] by using deuterium-enriched water and CH_4. Using the Arrhenius plot they determined the rates of exchange. The group concluded that a catalyst is vital for such exchange to occur, else, this reaction would require billions of years to occur at temperatures 125 °C and lower.

Isotopic exchange can occur not only between hydrogen isotopes, but also between oxygen isotopes. Experiments, that are based on isotopic exchange, can be used to determine the coefficient of diffusion. A diffusion model can be created and used to analyze the profiles of surface concentrations of oxygen isotopes over time [29]. However, Martin and Duprez [30] showed by experimenting with exchange of deuterium and OH groups, that hydrogen exchange occurs at lower temperatures than oxygen exchange.

Isotopic exchange is desirable not only for the above-mentioned applications, but also for the medical industry. Deuterium can be added to pharmaceutical drugs by hydrogen isotopic exchange. This process is very significant for such applications because incorporating deuterium atoms into drugs can act as a tool to study chemical and biological processes, limit drug degradation during metabolism, and study the metabolism of a specific medicament without changing the parent molecules. Iridium, ruthenium, rhodium, palladium, and platinum catalysts are used for these

applications; however, a catalyst should be chosen based on specific needs and molecules to achieve deuteration through isotopic exchange [31].

Methylmercury is a neurotoxin. It can form when mercury (Hg(II)) is affected by certain microorganisms – microbial methylation. This process depends on the interactions between Hg(II) and an ion or molecule attached to a metal atom, adsorption on minerals, as well as oxidation and reduction reactions. In real life, as well as laboratory conditions, mercury isotopes can be used to track methylation and demethylation processes, and a study by Zhang et al. [32] suggests that considering the process of isotopic exchange can help with making more accurate assessments of risk in relation to methylation, therefore, this process should not be overlooked.

Reaction rate is important when analyzing kinetics of heterogeneous catalysis processes. That is because a catalyst is used for the purpose of creating a favorable environment for a certain reaction to take place on. Arrhenius relation allows to express the dependence of reaction rate to temperature [27, 33]:

$$k = A \exp(-E_a / RT) \quad (2)$$

Where k - Reaction rate, A – pre-exponential factor, E_a – reaction activation energy, T – temperature. When modeling a process of heterogeneous catalysis, the reaction rate has to be determined.

Isotopic exchange experiments are significant because they can reveal information about the surface mobility, such as: the role of the promoter (if there is one), the role of the catalyst support, mobility of the isotopes, exchange mechanisms [34-37].

Precious metals, used in catalysts, are very expensive. To get the most use of the catalyst, the metal particles are small and well-dispersed on a support, most commonly with high surface area and high porosity [38, 39]. Dispersion can vary throughout the lifetime of the catalyst: metal particles may agglomerate due to elevated temperatures, which would decrease the dispersion, however, re-dispersion is sometimes possible, too, which would increase the dispersion [40]. This parameter has a big impact on the performance of the catalyst; therefore, it should be considered when creating a kinetic model.

2. Methodology

2.1. Kinetic modeling.

2.1.1. Experimental reference.

This work is computational. A computer code was written for the purpose of creating a kinetic model. Using "MATLAB" software and its programming language, a model for heterogeneous catalysis was created.

Kinetic modeling is based on the kinetics of a certain process. A set of differential equations describe the kinetics of certain variables. Solving these differential equations allows us to describe how these variables change over time.

This kinetic model describes the equilibration reaction with two hydrogen isotopes H_2/D_2 reacting, and forming the product HD [34]:

$$H_2 + D_2 \rightarrow 2HD \quad (3)$$

Processes that occur during the experiment that was conducted by García et al. [34] were identified: adsorption, desorption, and the equilibration reaction (see equation (2)). When creating a kinetic model for a specific case, such as this, when we have a ruthenium catalyst on a carbon support, it is important to also identify the properties they have.

Authors have described the influence of the pretreatment of the different samples. Pretreatment and promoters change the occurring processes. The processes, that we identified, apply to the sample we chose to analyze and recreate in the form of a kinetic model, however, other samples may also experience surface diffusion during the experiments the group [34] conducted.

Ruthenium-based catalysts on activated carbon supports were prepared with different percentage of mass of the noble metal, dispersion, particle size, as well as a different surface area of the activated carbon support.

Table 1. The parameters used in the kinetic model.

Parameter	**Value, units**
Volume of reactor (V) [34]	70 cm^3
Reaction rate (k)	$4.4 \cdot 10^5$ $m^2/mol \cdot s$
Weight fraction of Ru in the catalyst (f_{Ru}) [34]	2 %
Mass of the catalyst (m_{cat}) [34]	5 mg
Dispersion (D) [34]	41.2 %
Concentration of surface atoms of Ru (c_{Ru}) [39]	$1.63 \cdot 10^{19}$ m^{-2}
Molar weight of Ru (M_{Ru})	101.07 g/mol
Initial Partial Pressure of H_2 [34]	19 mbar
Initial Partial Pressure of D_2 [34]	19 mbar
Initial Partial Pressure of H_D [34]	0 mbar

The sample of Ru/AC_0 was pretreated at 300 °C under H_2 flow for 2 h, then outgassed under argon flow at 500 °C for 2 h and cooled in vacuum to 0 °C. A promoter was not added to this sample. Authors analyzed the changes of the partial pressure of H_2, D_2, and HD over time for this sample and stated that the only reaction taking place in this case was the isotopic equilibration reaction of H_2 and D_2 on the surface of the metal. On a theoretical level, this knowledge allowed to assume that the processes that occur in this case are adsorption, desorption, and the chemical reaction between the isotopes on the surface of ruthenium, and no hydrogen species of the support are participating in the isotopic exchange [34].

2.1.2. Theoretical reference.

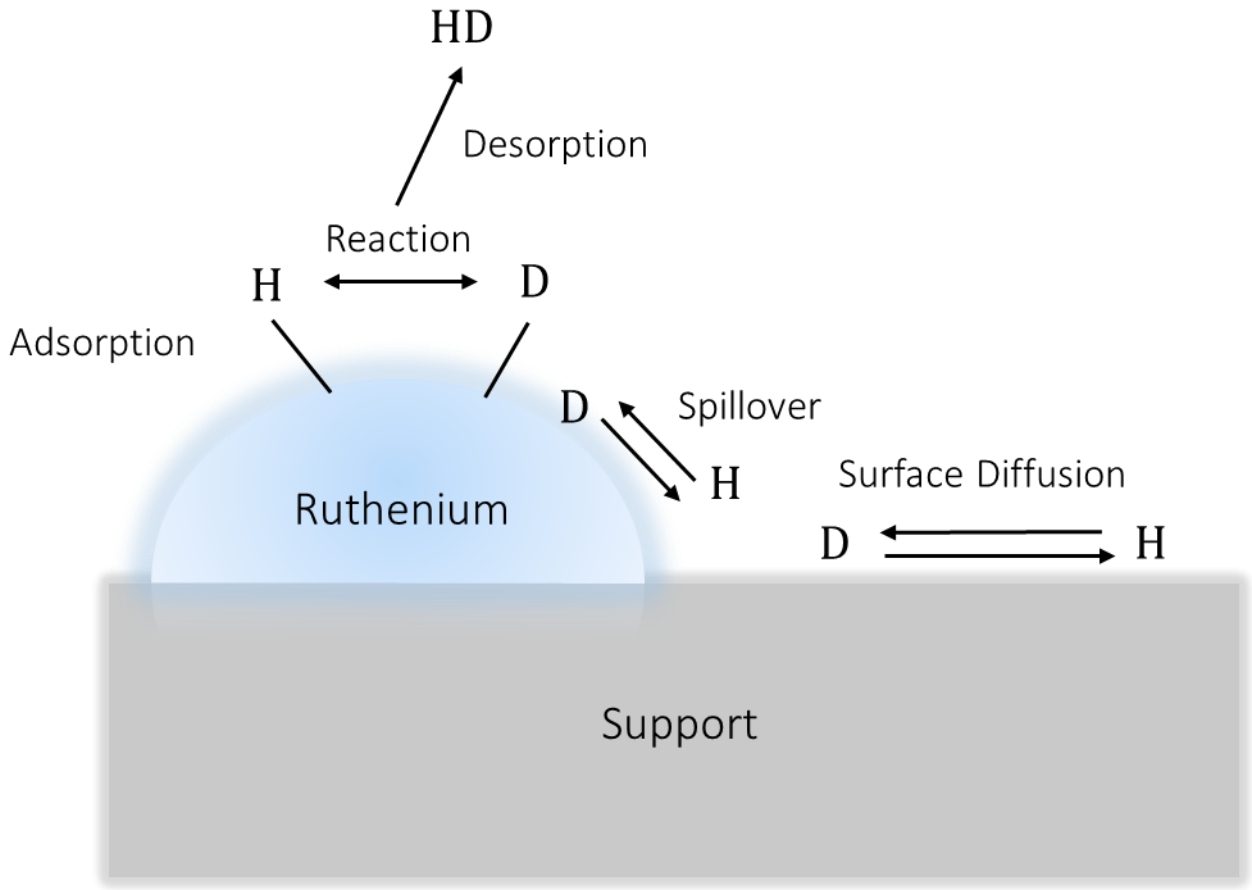

Figure 1. Interactions of hydrogen and deuterium between themselves, metal, and the support, adapted from [35] and applied to [34].

Once the reference experiment was chosen and information about it was gathered, the parameters of the process were collected, and the initial values were assigned in the "MATLAB" code. The values of necessary initial parameters were obtained from the literature (see Table 1).

In figure 1 we see which processes occur on the surface of a nanostructured catalyst. Adsorption of H and D on ruthenium allows the reaction to take place and form HD which then can desorb, leaving the metal available for other atoms to adsorb on. Atoms can spillover from the metal to the support, which continues in the form of surface diffusion. The visuals are based on a work of a similar nature [35]: the isotopic exchange of oxygen species was analyzed in their work; many parallels can be drawn between that work and our work with isotopic hydrogen exchange.

Automotive catalysts were analyzed [35] in a similar fashion as the catalysts for ammonia synthesis in the experimental reference [34] of this work. Graphs of partial pressure values over time for oxygen, and hydrogen isotopes, were presented in both works, as well as the isotopic exchange method was applied in both cases to observe the mobility of said isotopes on the surface of catalysts.

2.2. Building the code

2.2.1. Defining time

Time values play a key role in this model, in "MATLAB" can be described this way:

```
tPr = 0; % Time, the initial value.
tGal = 4000; % Time, the final value.
dt = 0.001; % Time step.
q = tGal/dt; % Defines the number of time values.
time = linspace(tPr,tGal,q); % Creates an array of time values.
```

An experiment [34] is used as a reference for the kinetic model. It is important to distinguish between the time values in the experiment, and in the code. The experiment, that is being referenced, lasts 500 seconds, however, here it appears that 4000 s are chosen instead. That is not exactly the case, there are a couple of reasons to do so.

The time values in the code can be considered dimensionless, they only define the number of iterations in a time cycle of the code. Choosing the time value that is higher than the number of seconds in the real experiment can be used to increase the number of iterations in the main cycle. While it was not a necessity in this work, this approach can be useful if we desire to increase the accuracy of the calculation.

Another reason to use this tactic is to make it easier to find the values of parameters that we are searching for, in this case, the reaction rate. When the time value is chosen to be higher or lower than the actual value of time, it helps us see how the results turn out over the period of time of our choice. An example of this approach is choosing a higher value of time (such as 4000) and guessing a reaction rate that is quite too low. Even though the reaction rate is too low, the process time is extended, therefore there is a chance to see if the results of the calculation appear to be similar to what is wanted, in contrast, using the true value (500 s) could return results that look nothing like what is expected, creating confusion and potentially resulting in "overfixing" of the code even though the mistake was not even there in the first place.

Manipulation of the time values can be useful, as mentioned above, however, it is crucial to be mindful of the changes it causes to the rest of the code. In this case, to make the dimensionless time units match the time units of the experiment (seconds), the final value would have to be divided by 8 using a new variable `x=time/8` so that each value in the time array could be considered to have the dimension of seconds. The number 8 is used in this case because we use 8 times more time units than in the experiment (4000/500=8), so it is important not to skip this step, unless `tGal` would match the number of seconds in the experiment. The reaction rate would also be impacted by this. In the code with 4000 time units, the reaction rate is written as being 8 times lower than the actual value, that is taken into account when drawing conclusions about the value of the reaction rate.

2.2.2. Initial calculations and parameters

The surface area of metal clusters is an important parameter for the calculations of the equilibration reaction between hydrogen and deuterium and for the surface diffusion. It is calculated [35]:

$$S_{Ru} = \frac{N_A f_{Ru} m_{cat} D}{c_{Ru} \cdot M_{Ru}} \tag{4}$$

where N_A[mol^{-1}] is the Avogadro's number; f_{Ru}[%] is the weight fraction of Ru in the catalyst; m_{cat} [g] is the mass of the catalyst; D[%] is the dispersion; c_{Ru}[m^{-2}] is the concentration of surface atoms of Ru; and M_{Ru}[g·mol^{-1}] is the molar weight of Ru.

The volume concentrations describe the amount of hydrogen isotopes H_2 and D_2, as well as the reaction product HD in the gas phase – in the volume of the reactor. The results of the experiment [34] are presented as values of partial pressure over time. The following equation allows us to make a connection between the pressure and the concentration of a certain molecule in the gas phase:

$$n_i = \frac{p_i}{k_B T}, \qquad i = H_2, D_2, HD \tag{5}$$

where n_i[m^{-3}] are the volume concentrations of H_2, D_2, HD molecules; p_i[Pa = kg·m^{-1}·s^{-2}] is the partial pressure of; k_B [J·K^{-1} = kg·m²·s^{-2}K^{-1}] is the Boltzmann's constant; T[K] is the temperature.

Equation (4) is used on two occasions in the code, first, to calculate the initial values of n_i. The numbers (1,1) indicate that the very first element of a certain array is used in the calculation. It can be observed, in the piece of code below, that equation (4) is divided by Avogadro's number.

```
nH2(1,1) = ( ( pH2(1,1) / (kb * T) ) ) / NA;

nHD(1,1) = ( ( pHD(1,1) / (kb * T) ) ) / NA;

nD2(1,1) = ( ( pD2(1,1) / (kb * T) ) ) / NA;
```

This practice reoccurs later in the code for the purpose of making the calculations easier for the computer to deal with. Applying equation (4) directly, forces the computer to perform calculations with numbers that are very big (e.g., 10^{23}) or very small (e.g., 10^{-23}), this requires more resources and can become problematic when using an average personal computer (which was the case in the making of this work). Dividing the formula by N_A brings the numbers closer to 1, however, additional attention must be paid to the dimensions everywhere in the code. The volume concentrations in the code are expressed in units of mol·m^{-3}.

The calculations in the main cycle require us to know the percentage of H_2, D_2, and HD at each moment in time. Initial conditions must be described before the main cycle. This will be explained in more detail later. For the initial fractions of molecules in the gas phase, as well as for calculating these values for other moments in time, we use:

$$f_i = \frac{n_i}{n_{H_2} + n_{HD} + n_{D_2}}, \qquad i = H_2, D_2, HD \tag{6}$$

For the first time moment we describe these fractions as such:

```
fH2(1,1) = (nH2(1,1))  / ((nH2(1,1) + nHD(1,1) + nD2(1,1)));

fHD(1,1) = (nHD(1,1))  / ((nH2(1,1) + nHD(1,1) + nD2(1,1)));

fD2(1,1) = (nD2(1,1))  / ((nH2(1,1) + nHD(1,1) + nD2(1,1)));
```

In the main cycle swap out the `(1,1)` for `(1,t)` to calculate these values for each moment in time.

2.2.3. Surface concentrations and diffusion

Surface concentrations of hydrogen and deuterium atoms are not only important for the calculation of the isotopic equilibration reaction process, but also for the surface diffusion, therefore, the initial values and arrays describing these surface concentrations include not only time, but also the surface layers. It will become clearer why that is important later in this chapter. An example of the initial arrays is provided below:

```
cH = zeros(1,length(time), length(layers));

cD = zeros(1,length(time), length(layers));
```

This means that these arrays will have as many elements as time values multiplied by the number of layers. Initially all these values are set to be zero, the surface concentrations during the first value of time are not specified further in the code, which means that the very first value of these surface concentrations of hydrogen and deuterium atoms are zero. It does not have to be zero in all cases, for example, if we know that a certain amount of hydrogen is already present on the surface, that value can be set to be the first one. Setting the values to zero in the code means that we see the experiment in such a way that in the first moment in time we have absolutely no H and D on the surface of the catalyst.

The main cycle runs based on the time values (`for t = 2:length(time)`). The cycle starts at the second value of time, this is because of the way the equations in the cycle are written. Previous time moment `t-1` is often used, which means if the cycle would start at the first time moment, it would not be possible to calculate as “MATLAB” does not have arrays with the 0-th element, instead, all arrays start with the 1-st element. This further explains why the initial values are chosen before the cycle. For example, the fractions of molecules in the gas phase are calculated using the same equation for the very first value, as well as the rest of them (see equation (5)), however it is not possible to include the calculation of the initial value in the main cycle. There might be ways to do it in “MATLAB” or using a different programming language, however, a completely different approach might be required for building the entire code.

The equations in the main cycle describe adsorption, desorption, the equilibration reaction, and surface diffusion. First, it is important to understand how the surface diffusion is described in this work. The word “layers” has already been mentioned above, now it will be explained further. In the code, surface diffusion is first described by introducing the layers into the already existing code like this:

```
iPr = 1; %Layer, the number of the first layer.
dh = 1*10^-9; %Layer thickness.
SC0 = 960; % The surface area of the support.
d = 2.7 * 10^-9; % The size of one metal particle.
NRu = (SRu / (5 * d * d) ); % Total number of Ruthenium particles.
xRu = ((Sc0 / NRu)^(1/2)); % The distance between Ruthenium particles
```

```
iNumber = 0.5 * xRu / dh; % The total number of layers.
layers = (1:1:inumber); % Array of layer numbers.
```

To generate the array of layer numbers, first we must know the number of ruthenium particles on the surface of the catalyst [27, 35]:

$$N_{Ru} = \frac{S_{Ru}}{5d^2} \tag{7}$$

here N_{Ru} – the number of ruthenium particles on the surface of the catalyst; d[m] is the size of one ruthenium particle.

Then the distance between ruthenium particles was calculated [27, 35]:

$$x_{Ru} = \sqrt{\frac{S_{C0}}{N_{Ru}}} \tag{8}$$

here x_{Ru}[m] – the distance between ruthenium particles and S_{C0}[m^2] is the size of one ruthenium particle.

Finally, the total number of layers was obtained [27, 35]:

$$i_{Number} = \frac{0.5 \cdot x_{Ru}}{dh} \tag{9}$$

Here dh[m] is the thickness of a layer.

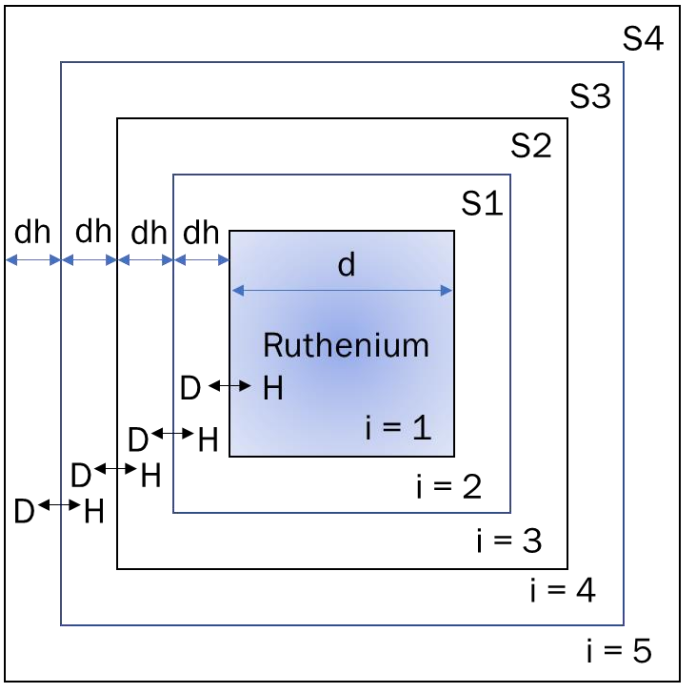

Figure 2. Surface diffusion of hydrogen and deuterium, adapted from [36].

The array of layer numbers is created as showed in the code piece above. The array contains the number of layers from the first layer `iPr` first to the last layer (which we know because the total number of layers was calculated) with the step of one, like `layers = [1 2 3 4 5……iNumber]`.

Figure 2 shows the layers that were just described. Ruthenium particle in the center is square-shaped. Ruthenium is on an activated carbon support which is divided into square-shaped layers of dh width. Spillover and reverse spillover from and to the metal and subsequent diffusion occurs. Although the thickness of the layers is the same for each layer, the surface area is not, as it is increasing in size the further the layer is from the ruthenium particle. The change of the surface area is significant enough to account for that in our calculations [35, 36]:

$$S_{Layer}(i_{Number}) = 4 \cdot N_{Ru} \cdot dh \cdot (d + (i_{Number} - 2) \cdot dh) \quad (10)$$

This formula is applied in the code by creating a tiny `for` cycle that calculates the surface area by performing as many iterations as there are layers, leaving us with an array with the surface area values for each of these layers:

```
for i = layers(1:end)

        Slayer(1,i) = 4 * N * dh * ( d + (i-2) * dh );

end
```

The spillover and reverse spillover are both important when including the surface diffusion in the code. It is considered that H and D atoms can move from the ruthenium particles to the surface of the support, as well as from the support to the ruthenium particles. In the code we explain these processes as if they were connected: if one atom experiences spillover from Ru to the support, then another atom will experience the reverse spillover from the support to the metal particle [35, 36].

$$\left(\frac{dc_D^1}{dt}\right)_{Spill} = -\frac{D_s}{dh^2} \cdot (c_D^1 - c_D^2) \cdot A^1 = -\left(\frac{dc_H^1}{dt}\right)_{Spill} \quad (11)$$

Here c_D^1 and c_H^1[mol·m^{-2}] are the surface concentrations of deuterium and hydrogen, respectively. The number in superscript denotes the number of the layer: 1 means the concentration is calculated on ruthenium, 2 means the first layer of support. D_s[m^2·s^{-1}] is the diffusion coefficient. A^1 is a coefficient that describes the direction of the flux of diffusing atoms and accounts for the surface area of different layers, as already mentioned, these surface areas increase the further the layer is from the ruthenium particle.

In the code the spillover process impacts the surface concentrations in every moment of time and in the first layer:

```
cDSD(1,t,1) = -(Ds/(dh * dh))*( cD(1,t-1,1) - cD(1,t-1,2) ) * A(1,1);

cHSD(1,t,1) = -cDSD(1,t,1);
```

Coefficient A^i is calculated differently depending on the surface concentrations [35, 36]:

$$A^i = \begin{cases} \frac{S^{i+1}}{S^i}, & if\ c_j{}^{(i)} - c_j{}^{(i+1)} \geq 0 \\ \frac{S^i}{S^{i+1}}, & if\ c_j{}^{(i+1)} - c_j{}^{(i)} < 0 \end{cases}, \qquad j = H, D \tag{12}$$

Diffusion cannot occur without describing adsorption in this work. The effect adsorption has on surface concentrations c_D^1 and c_D^1 is such that the adsorbed atoms increase the surface concentration of H or D on ruthenium. Adsorption's influence on the surface concentration over time is calculated like this [35, 36]:

$$c_H(t) = \left(f_{H_2}(t-1) + \frac{1}{2} f_{HD}(t-1)\right) \cdot (c_{Ru} - \left(c_H(t-1) + c_D(t-1)\right) \tag{13}$$

$$c_D(t) = \left(f_{D_2}(t-1) + \frac{1}{2} f_{HD}(t-1)\right) \cdot (c_{Ru} - \left(c_H(t-1) + c_D(t-1)\right) \tag{14}$$

Here c_{Ru}[m^{-2}] is the concentration of surface atoms of Ru. Fractions f of H_2, HD and D_2 define how much of hydrogen or deuterium is available in the gas phase, as they have the potential to adsorb on the metal. Multiplying the fraction of HD by $\frac{1}{2}$ is necessary because only half of HD consists of H (see equation (12)), and half of D (equation (13)). The second part of these equations show the metal sites that are available for H and D (equations (12) and (13), respectively), because c_{Ru} shows all the available sites before the process began, and the sum of $c_H(t-1)$ and $c_D(t-1)$ shows how many adsorption sites were already occupied by H and D in the previous time moment $(t-1)$. Adsorption occurs only in the first layer – the ruthenium site. In the code, these adsorption calculations are performed in the main time cycle, also setting the layer number to 1:

```
cHAD(1,t,1) = (fH2(1,t-1,1)+0.5*fHD(1,t-1,1))*(cRu-(cH(1,t-1,1)+cD(1,t-1,1)));

cDAD(1,t,1) = (fD2(1,t-1,1)+0.5*fHD(1,t-1,1))*(cRu-(cH(1,t-1,1)+cD(1,t-1,1)));
```

Another thing that influences surface concentrations is the chemical reaction between hydrogen and deuterium with the product HD.

$$c_H(t) = -k \cdot c_H(t-1) \cdot \left(c_H(t-1) + c_D(t-1)\right) \tag{15}$$

$$c_D(t) = -k \cdot c_D(t-1) \cdot \left(c_H(t-1) + c_D(t-1)\right) \tag{16}$$

Here k[$m^2 \cdot mol^{-1} s^{-1}$] is the reaction rate. The minus sign in equations (14) and (15) shows that the surface concentration of H and D, respectively, decreases because of the chemical reaction, because the product HD forms, using H and D. As the product forms, it desorbs from the metal. In the code we treat this piece of calculations similarly like we treated adsorption – this also only occurs in the first layer [35, 36]:

```
cHRE(1,t,1) = ( -k * cH(1,t-1,1) ) * (cH(1,t-1,1) + cD(1,t-1,1) );

cDRE(1,t,1) = ( -k * cD(1,t-1,1) ) * (cD(1,t-1,1) + cH(1,t-1,1) );
```

Generally, this kinetic model is created to simulate the process of hydrogen isotopic exchange phenomena, this experimental method has been used in the experiments that have been referenced, therefore, hydrogen and deuterium are considered in this work. The specific properties (e.g., mass) of neither of those are considered in this model, due to only fluxes being considered. However, the chemical reactions are described in the model as they are in real life, which has an impact on the result. Therefore, we must know what types of materials interact with each other and what type of a chemical reaction takes place.

The processes that influence surface concentrations were discussed above, namely, spillover, adsorption, desorption, and a chemical reaction. These processes occur in the first layer (ruthenium site) and the equations (10-15) together constitute the final equations of $c_H(t)$ and $c_D(t)$:

```
cH(1,t,1) =  cH(1,t-1,1) + cHAD(1,t,1) + cHRE(1,t,1) * dt + cHSD(1,t,1) * dt;

cD(1,t,1) =  cD(1,t-1,1) + cDAD(1,t,1) + cDRE(1,t,1) * dt + cDSD(1,t,1) * dt;
```

The concentration of the current moment in time `t` is calculated by first taking the value of `c` in the previous moment in time `t-1`, then adding the adsorption, chemical reaction/desorption multiplied by the time step, and surface diffusion multiplied by `dt`. We do not multiply for the adsorption because it is an instantaneous process [27].

Now that the diffusion is included in the first layer, it is time to include it in all the other layers. If an atom jumps from the metal to the support, it further diffuses. In our case, it is known [34] that the support can have some H species and no D species initially. It was already mentioned that during spillover D moves from the metal to the support, the flux of D is compensated by the H flux of the opposite direction, this applies to all the layers.

$$\left(\frac{dc_D^i}{dt}\right)_{Dif} = -\frac{D_s}{dh^2} \cdot A^i\left(c_D^{i-1} - c_D^i\right) = -\left(\frac{dc_H^i}{dt}\right)_{Dif} \tag{17}$$

The code is written similarly like it was written for the spillover, however, here the equation (16) is slightly different from the equation (10), and we must swap out the `(1,t,1)` for `(1,t,i)`.

The final `cH` and `cD` equations are similar to the ones written for the first layer, however, we consider that adsorption and the chemical reaction do not occur on the support, therefore:

```
cH(1,t,i) = cH(1,t-1,i) + cHSD(1,t,i) * dt ;

cD(1,t,i) = cD(1,t-1,i) + cDSD(1,t,i) * dt ;
```

2.2.4. Volume concentrations and partial pressure

Now the surface diffusion, in terms of the surface concentration, has been described. However, the goal was to create a kinetic model that can provide results in terms of partial pressure. The previous steps were necessary to achieve that because surface concentration plays an important role in the calculations of volume concentrations, and these can be transformed into partial pressures using (4) equation. The steps to reach this goal are explained below.

Volume concentrations consist of two sets of equations, the first set defines how is adsorption related them, the second set defines the influence of the chemical reaction.

The adsorption component is expressed like this [35, 36]:

$$n_j = \frac{s_{Ru}}{2V} \cdot (c_{Ru} - \big(c_H(t-1) + c_D(t-1)\big) \cdot f_j(t-1), \qquad j = H_2, D_2, HD \qquad (18)$$

As the atoms adsorb on the metal the surface concentrations on the metal sites for these atoms will increase, however, for the gas phase it means that the same amount must be subtracted from the volume. This component will be subtracted in the general volume concentration equation. Adsorption in the code is written in the main cycle, only concentrating on time values, not iterating for each layer.

```
nH2AD(1,t) = ((SRu/(2*V)) * ((cm - (cH(1,t-1,1) + cD(1,t-1,1))) * fH2(1,t-1))) ;

nHDAD(1,t) = ((SRu/(2*V)) * ((cm - (cH(1,t-1,1) + cD(1,t-1,1))) * fHD(1,t-1))) ;

nD2AD(1,t) = ((SRu/(2*V)) * ((cm - (cH(1,t-1,1) + cD(1,t-1,1) ))* fD2(1,t-1))) ;
```

The chemical reactions also play a role in the volume concentrations. When the reactions occur on the ruthenium site, the reaction product desorbs from it into the gas phase, therefore, to keep the balance, this term is expressed like this [27]:

```
nH2RE(1,t) = ( SRu/(2*V) ) * k * (cH(1,t-1,1) * cH(1,t-1,1));

nHDRE(1,t) = ( SRu/ (V)  ) * k * (cH(1,t-1,1) * cD(1,t-1,1));

nD2RE(1,t) = ( SRu/(2*V) ) * k * (cD(1,t-1,1) * cD(1,t-1,1));
```

Finally, the main equation for the volume concentrations is obtained:

```
nH2(1,t) =    nH2(1,t-1)  + (nH2RE(1,t)) * dt - nH2AD(1,t);

nHD(1,t) =    nHD(1,t-1)  + (nHDRE(1,t)) * dt - nHDAD(1,t);

nD2(1,t) =    nD2(1,t-1)  + (nD2RE(1,t)) * dt - nD2AD(1,t);
```

Notice how the chemical reaction component is added and multiplied by the time step, and the adsorption is subtracted. And lastly, we obtain the partial pressure values by using the volume concentrations.

```
pH2(1,t) =  ( (nH2(1,t) * NA ) * kb * Tkamb);

pHD(1,t) =  ( (nHD(1,t) * NA ) * kb * Tkamb);

pD2(1,t) =  ( (nD2(1,t) * NA ) * kb * Tkamb);
```

The partial pressure values are obtained in Pa, they were converted to mbar in the “Results” chapter.

3. Results

A kinetic model for isotopic hydrogen exchange on a ruthenium-based catalyst was created based on the experimental data by Garcia et al. [34]. The code was built using the methodology explained in the chapter above. To check if the code is not only functional, but also reliable for analyzing the effect that different parameters have on the changes in composition of isotopic hydrogen in the gas phase, the values that were calculated using the "MATLAB" code had to be checked if they match the experimental data. This was done by plotting the experimental curves along with the calculated values of partial pressure of hydrogen, deuterium, and their reaction product HD over time to recreate the experimental curves (see Figure 3). When the simulation provides results that are satisfactory, in terms of fitting well with the experimental ones, the kinetic model can be used to analyze the influence of different parameters.

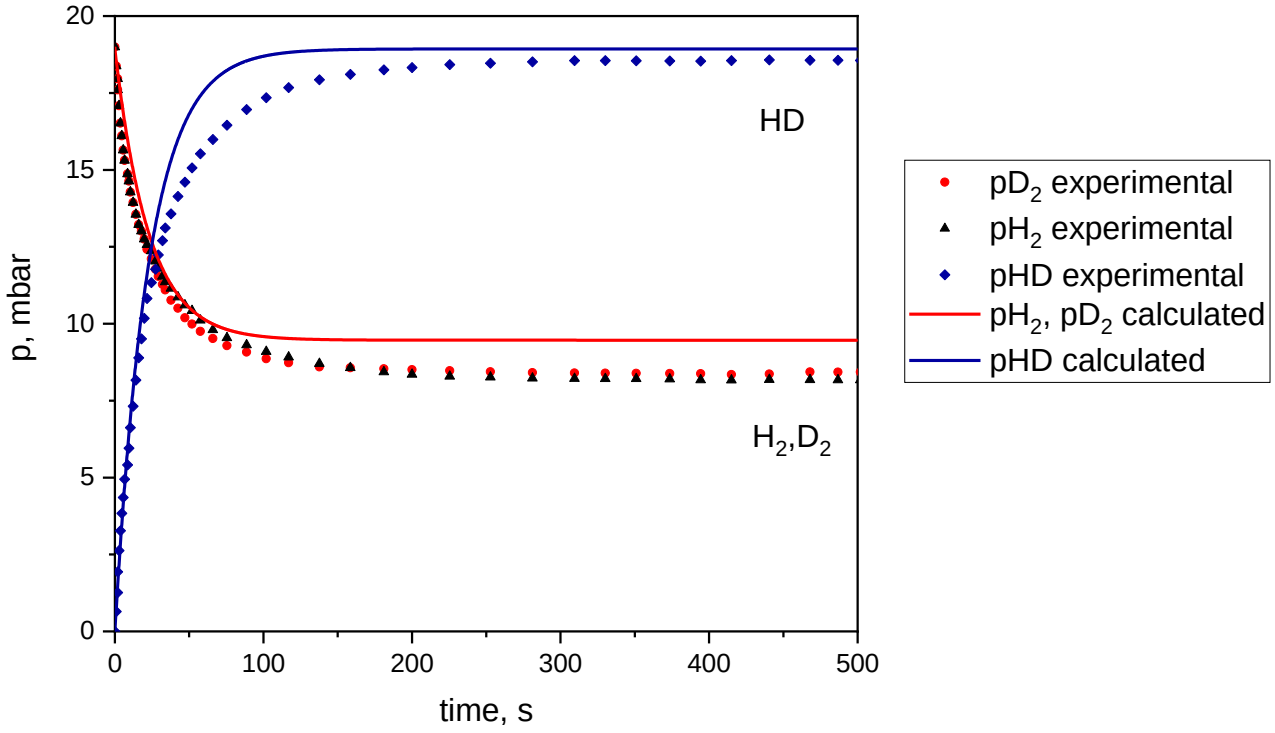

Figure 3. Experimentally [34] and theoretically obtained curves of partial pressure of hydrogen (pH_2), deuterium (pD_2), and hydrogen product (pHD) over time during the isotopic hydrogen exchange on Ru/AC catalyst.

The experimental values along with the calculated values of partial pressure over time were plotted to see how well-fitting the calculated curves are (Figure 3). Experimental and theoretical values are in nearly perfect agreement for the first 25s of the process. The HD production after the 25s mark turns out to be slightly faster in the theoretical curve than in the experiment. However, the curves reach a good agreement towards the end of the graph where the HD pressure stabilizes. Experimental values for hydrogen and deuterium content are almost perfectly aligned with each other. It matches perfectly in the theoretical calculations. As H_2 and D_2 values stabilize at around the 100s mark, the experimental and calculated curves begin differing slightly and the consumption of these isotopes is shown to be lower than in the experiment.

In the beginning of the experiment (as well as in our kinetic model) the initial inlet pressure of hydrogen and deuterium was 19 mbar for each isotope. That being the case, the pressure curves for the reactants are nearly the same in the experiment, and identical in calculations, as the equations that govern the evolution of the gas phase content for them are identical if no other parameters are changed. The reason for the consumption of these gases is the same for both isotopes is that initially equal amounts of these gases are inlet into the reaction chamber, and the catalyst was pretreated using hydrogen flow and argon flow for two hours individually, at elevated temperatures of 300 °C and 500 °C, respectively. This thermal pretreatment under argon at 500 °C ensures that there are no remaining hydrogen atoms on the surface of the catalyst, meaning that no reverse spillover can occur. However, if that was the case, this effect would show up in the graph in the form of higher D_2 consumption, and lower H_2 consumption, because H_2 could be "borrowed" from the support, instead of an external source [34].

Overall, the test model shows good agreement, therefore, going further, it is used to analyze the effect different parameters have on the system, starting with the influence of the reactor's volume (see Figure 4).

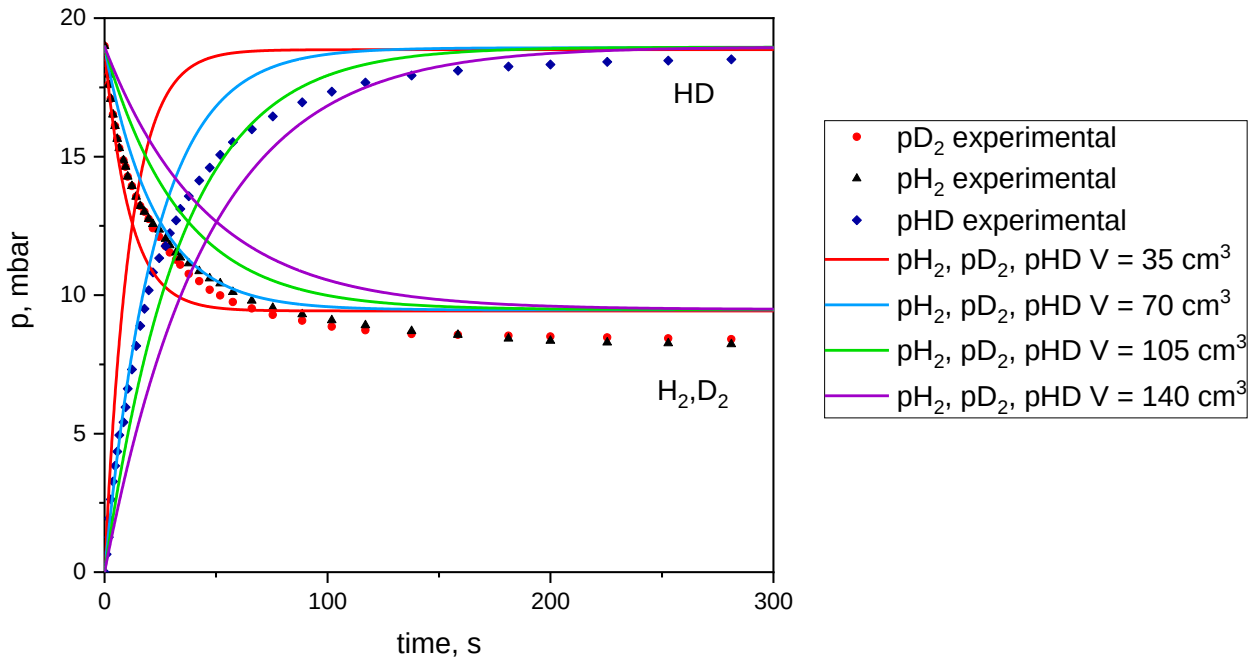

Figure 4. The influence of varying reactor volume values on the partial pressure during the isotopic equilibration reaction.

The value for the volume of the reactor in the experiment was V = 70 cm^3, other values were chosen to be 0.5, 1.5, and 2 times the initial volume. The higher the volume is, the slower the reaction occurs, as the distance between the particles is higher and particles are less likely to interact. Not to neglect the fact that the surface area of the catalyst remains the same, which makes the process slower as the same surface area must deal with a different volume of the reaction chamber, the distance each particle must travel to interact with the catalyst changes. Therefore, in figure 4 the red curve, which represents the pressure at the lowest reactor volume, is so steep in the first 12.5 seconds. The points

at which HD production is equal to the H_2 and D_2 consumption are positioned at equal distances: from V = 35 cm^3 to V = 70 cm^3, from V = 70 cm^3 to V = 105 cm^3, and from V = 105 cm^3 to V = 140 cm^3. This means that the time in which the reaction occurs depends on the volume, the production/consumption point equalizes by a ratio of 2.8 if we were to divide the volume by the time it takes to reach the equalization point, as such:

$$\frac{V}{t} = \frac{35}{12.5} = \frac{70}{25} = \frac{105}{37.5} = \frac{140}{50} = 2.8 \tag{19}$$

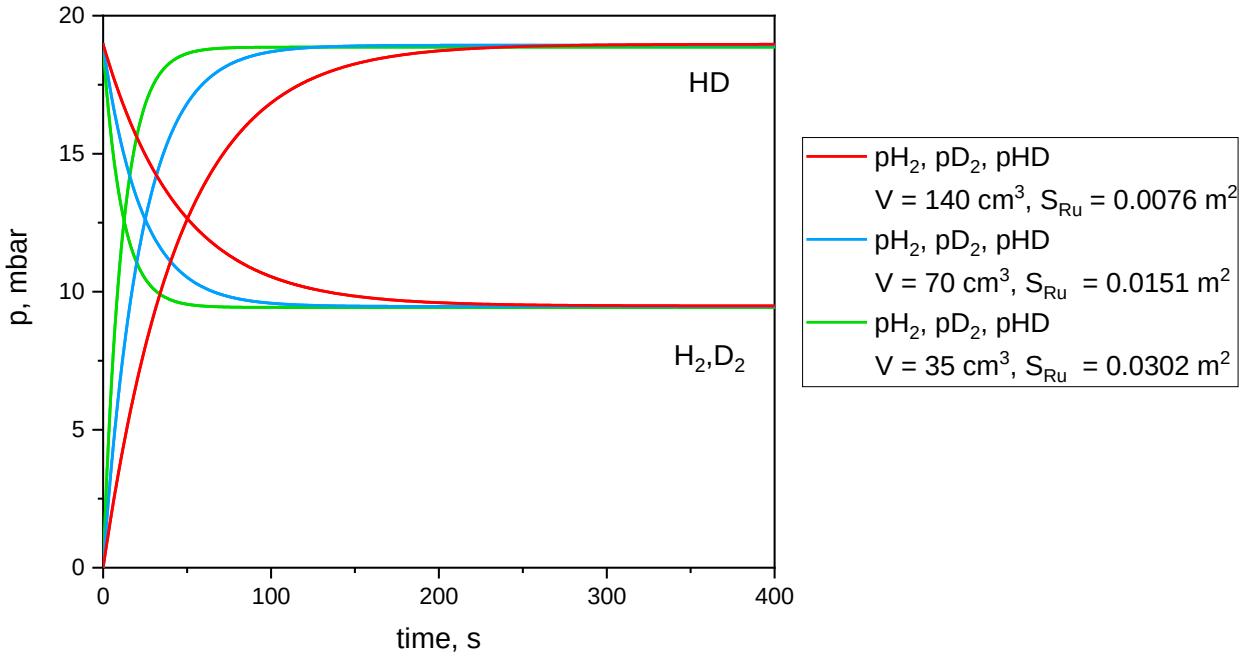

Figure 5. Theoretically obtained curves of partial pressure of hydrogen (pH_2), deuterium (pD_2), and hydrogen product (pHD) over time during the isotopic hydrogen exchange on Ru/AC catalyst and the influence of varying reactor volume values and the surface area of ruthenium on the partial pressure during the isotopic equilibration reaction.

The influence of the reactor's volume is directly related to the already mentioned surface are of ruthenium (see figure 5). These parameters are inversely proportional:

$$\frac{V_1}{V_2} = \frac{140\ \text{cm}^3}{70\ \text{cm}^3} = \frac{S_{R2}}{S_{R1}} = \frac{0.0151\ \text{m}^2}{0.00755\ \text{m}^2} = 2 \tag{20}$$

In figure 5 the graphs are portrayed in a way to show that manipulating the parameters of volume and surface area of ruthenium gives the same result if it is done according to the proportions. In other words, increasing the surface area of ruthenium will give us the same result as increasing the volume of the reactor.

The graph in red shows pHD, pH_2, pD_2 changes over time, in fact, it is not just one graph but two, perfectly aligned on top of each other. It shows that if the volume of the reactor is increased from the baseline volume (70 cm^3) to be twice as large (140 cm^3), it is the equivalent of reducing the surface area of the noble metal by half (0.0148 m^2 / 2). The idea is the same for the green and the blue graphs.

The reactor might not be as easy to change in a laboratory, it might be easier to achieve the same result by changing the surface area of the noble metal on a catalyst. This is also useful to know in modeling a process like the one in this work because these parameters will change the outcome in the same manner, however, inversely.

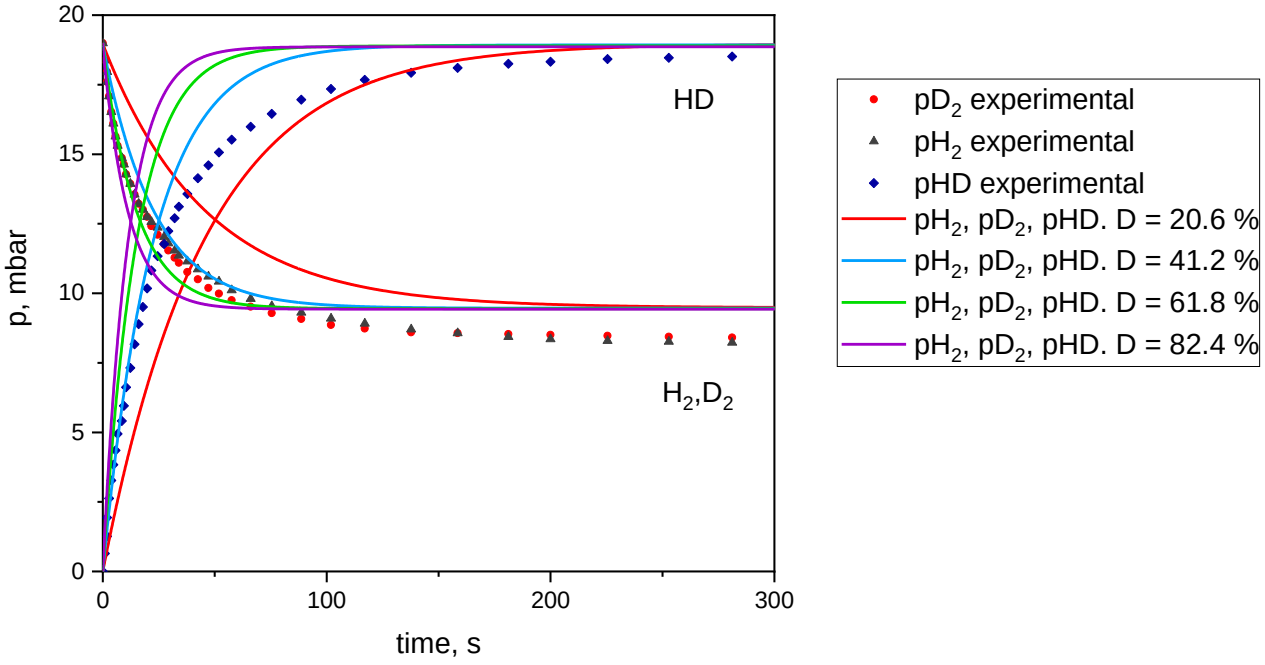

Figure 6. The influence of varying levels of ruthenium dispersion on the partial pressure during the isotopic equilibration reaction.

Dispersion of the ruthenium particles was analyzed (see Figure 6). Dispersion defines a ratio of ruthenium atoms that are on the surface of the catalyst to the total amount of these atoms (see Figure 7).

When a catalyst is repeatedly used, there is a tendency for the particles to aggregate, which is problematic in the long run, as the catalyst becomes less effective over time. To show the effect it has on the isotopic hydrogen equilibration reaction, calculations were made with different dispersion values.

The way particle size is related to dispersion, if the metal particle is considered to be cubic, was shown in Ref. [23], where we see these are inversely proportional:

$$d = \frac{M_{Ru}}{D\rho_{Ru}a_{Ru}N_A} \cdot 10^2(nm) \qquad (21)$$

Where M_{Ru} – article atomic mass of ruthenium; D – dispersion; ρ_{Ru} – bulk density of Ru [g·nm^{-3}]; a_{Ru} – atomic area of Ru atom [nm^2·atom^{-1}]; N_A – atomic Avogadro's number [mol·atom^{-1}].

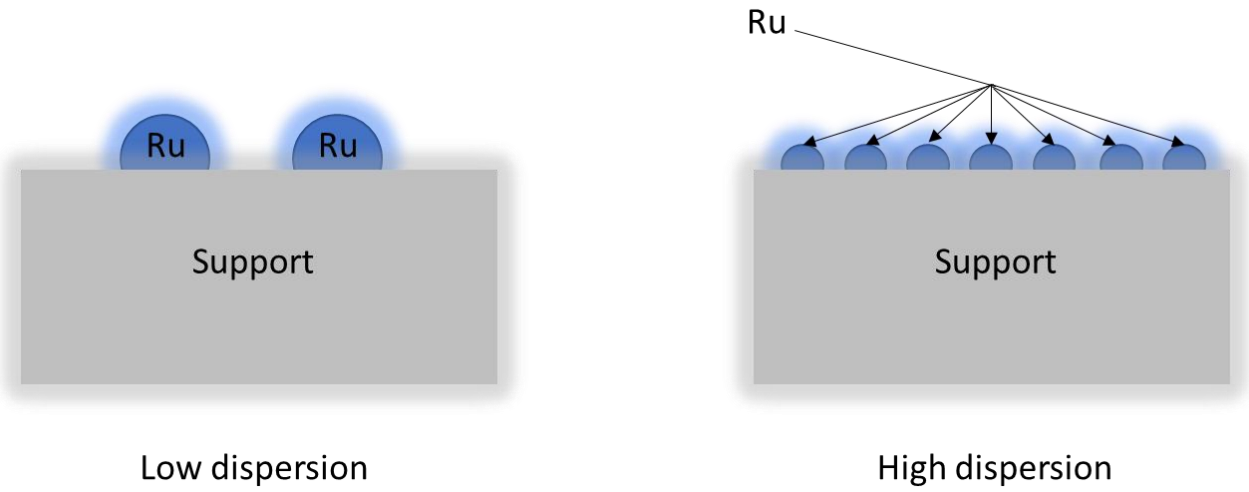

Figure 7. Hypothetical scenario visualizing the concept of a low and high level of noble metal particle dispersion, adapted from [40].

In Figure 6 we see that having a catalyst with higher dispersion values results in the reaction reaching its stability faster than for those that have lower dispersion values. The production of HD reaches the point of equalizing with H_2 and D_2 consumption in the first 12.5 seconds for 81.4% dispersion, however, takes around 50 seconds to do that for 20.6 % dispersion. These time points t are inversely proportional to dispersion D. In this case decreasing dispersion 4 times results in needing 4 times longer for the reaction to reach the crossing point between the partial pressure of the reactants and the product:

$$\frac{t_1}{t_2} = \frac{12.5\ s}{50\ s} = \frac{D_2}{D_1} = \frac{20.6\%}{81.4\%} = \frac{1}{4} \tag{22}$$

Dispersion influences the surface area of ruthenium particles (see Equation (3)). Dispersion relates to the particle size. Experimental results of Ref. [34] also show this tendency of partial pressure reaching stable values faster when the dispersion values are higher.

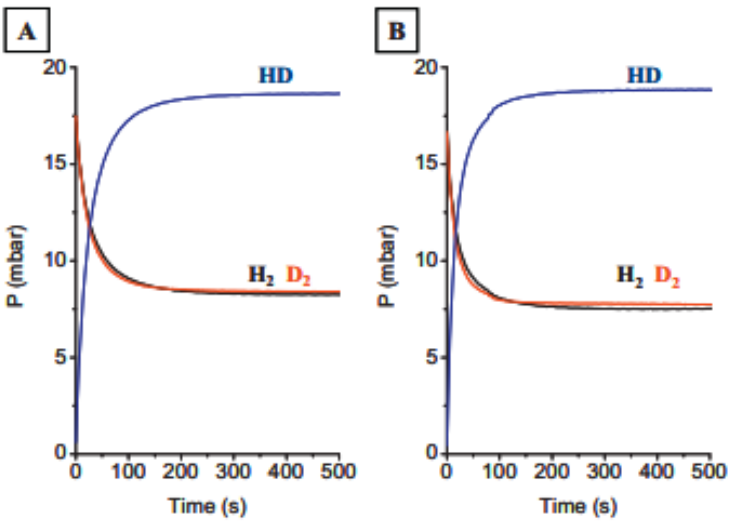

Figure 8. Partial pressure over time. A) Dispersion 41.2%. B) Dispersion 56.2% [34].

In Figure 7, scenarios of low and high dispersion are visualized: on the left we see low dispersion, meaning that the noble metal is possibly aggregated and forms bigger particles, less surface area is available for the reaction to take place on so the process of the heterogeneous catalysis becomes slower as the reactants have only that much space to interact with each other and form HD which then has to desorb from the metal to allow other atoms to adsorb and continue the catalytic cycle; on the right we see highly dispersed particles of lower diameter, this can be achieved by hydrothermically treating a catalyst [40] in the case of Pd-based catalysts for CO oxidation, or simply the catalyst can be prepared in a good enough way that it does not significantly aggregate over the course of its lifetime.

Researchers are looking into various ways to improve existing catalysts by using dispersion as a tool to achieve better catalytic activity. The interest for 100% dispersion catalysts is increasing as it would allow to make us of all the noble metal particles in the catalyst, these metals are very expensive, so successful development of such catalysts could reduce the overall price of the catalyst. However, it is challenging as metal atoms tend to agglomerate so the problem of maintaining this high level of dispersion is not to be ignored.

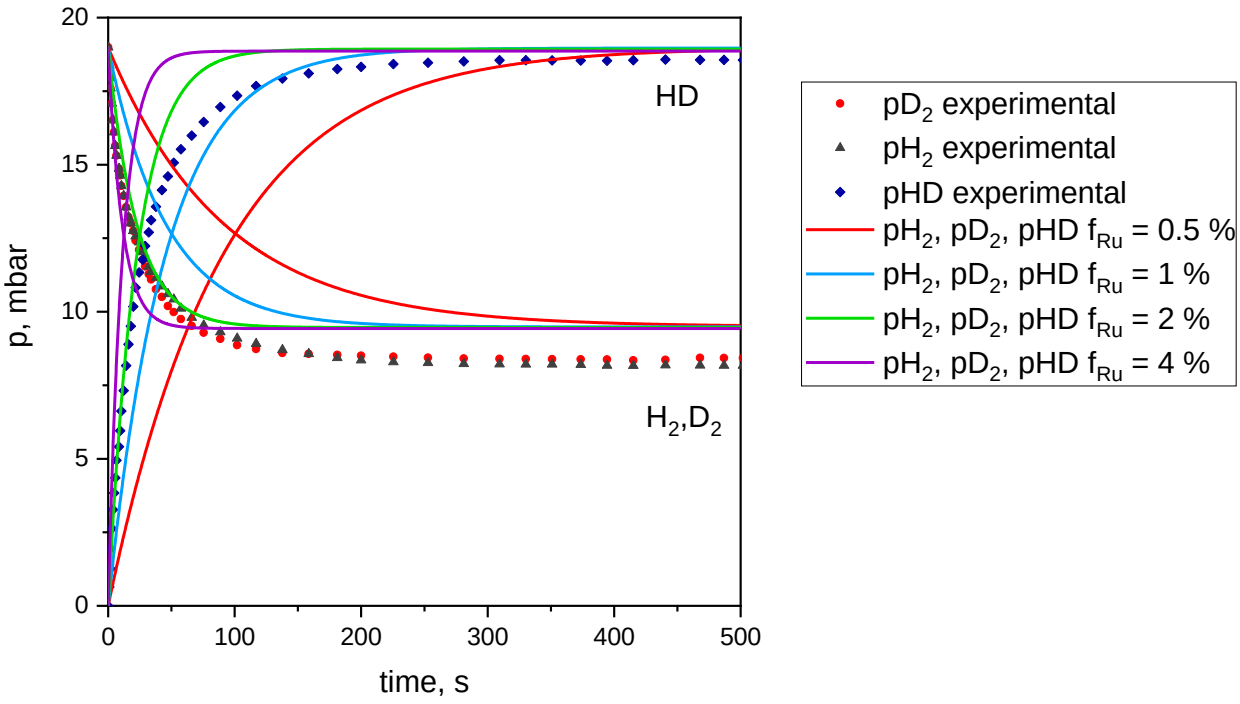

Figure 9. The influence of the fraction of ruthenium used in the catalyst on the partial pressure during the isotopic equilibration reaction.

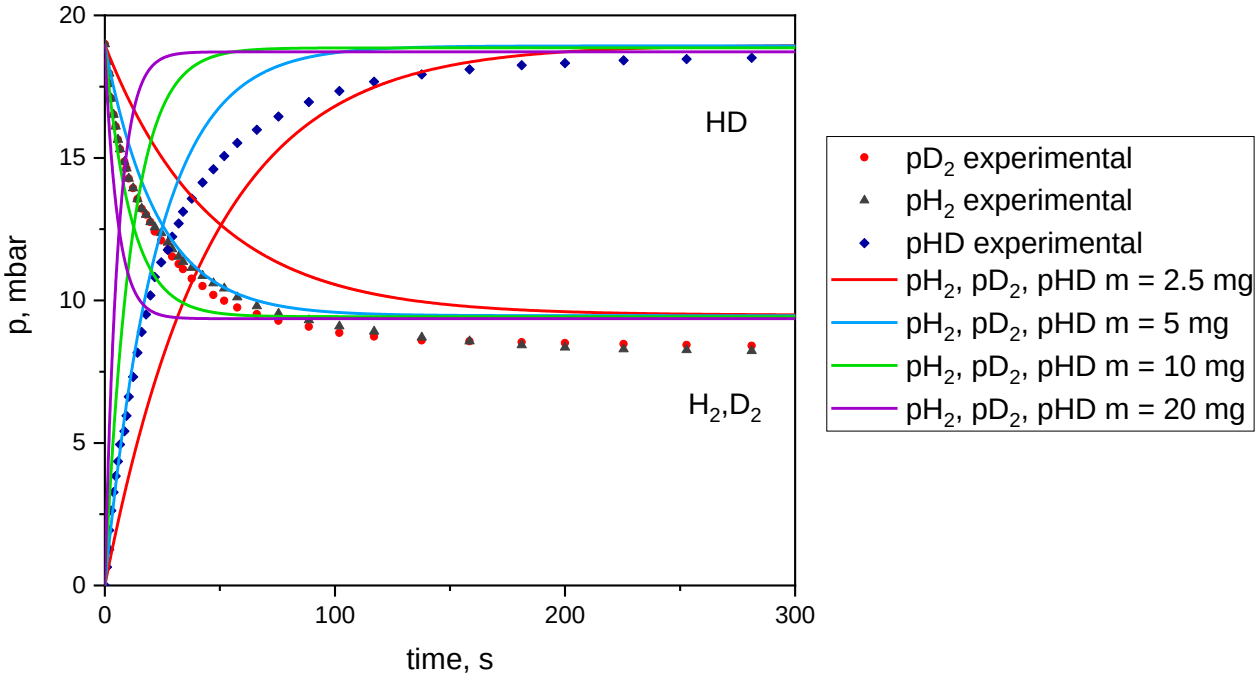

Figure 10. The influence of the mass of ruthenium on the partial pressure during the isotopic equilibration reaction.

The fraction of ruthenium in the catalyst (see Figure 9), as well as the catalyst mass (see Figure 10), have a very similar effect as dispersion: these parameters are both directly proportional to the surface area of the noble metal in the catalyst.

Logically, preparing the catalyst with a higher percentage of noble metal allows for quicker reactions as the surface area inevitably increases if more of the ingredient is used.

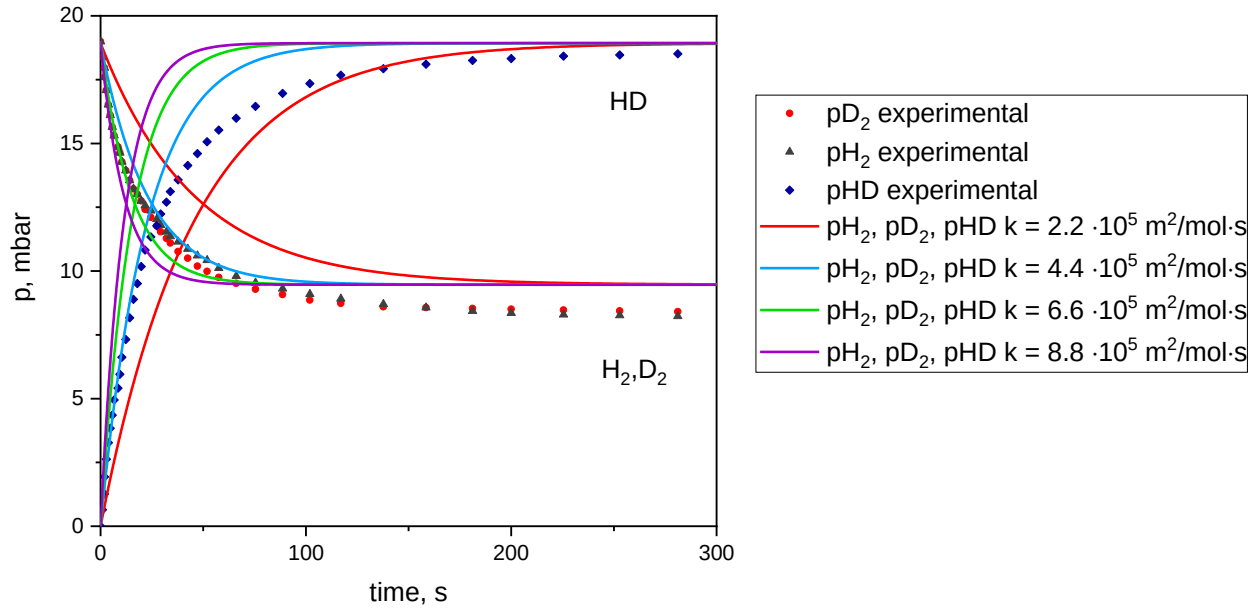

Figure 11. The influence of the reaction rate of the isotopic equilibration reaction on the partial pressure.

The initial challenge when fitting the experimental curves and the theoretical ones is that the appropriate reaction rate needs to be guessed in order to analyze the parameters further. The reaction rate was determined in the very beginning and used to achieve the result in Figure 3, in this case it was $4.4 \cdot 10^5$ $m^2 \cdot mol^{-1} s^{-1}$. To show the influence of this parameter, different reaction rates were chosen, and the results are provided in Figure 11. We can see that the higher the reaction rate is, the faster the system approaches a steady state regime.

All the parameters, which were analyzed up until this point, are based on the scenario where the initial pressure of hydrogen and deuterium is the same, and equal to 19 mbar for each. To show, that this kinetic model can be used to analyze situations where this parameter is different each hydrogen isotope, calculations have been performed for four cases. Experimental results were used in all cases to serve as a guideline. First graph (red) shows the main case where both H_2 and D_2 start off with 19 mbar. Blue graph shows the case where we lower the initial pressure of hydrogen to 15 mbar. Less HD is produced, less H_2 and D_2 is consumed compared to the results in graph a). Lowering the initial amount of hydrogen to 1 mbar results in even more significantly reduced HD production because only a small amount of H is available for the HD production (figure 12 c)). If the initial amount of hydrogen and deuterium is the same but higher than the one used in the experiment, such as 22 mbar for both, we see that it increases the overall consumption and production.

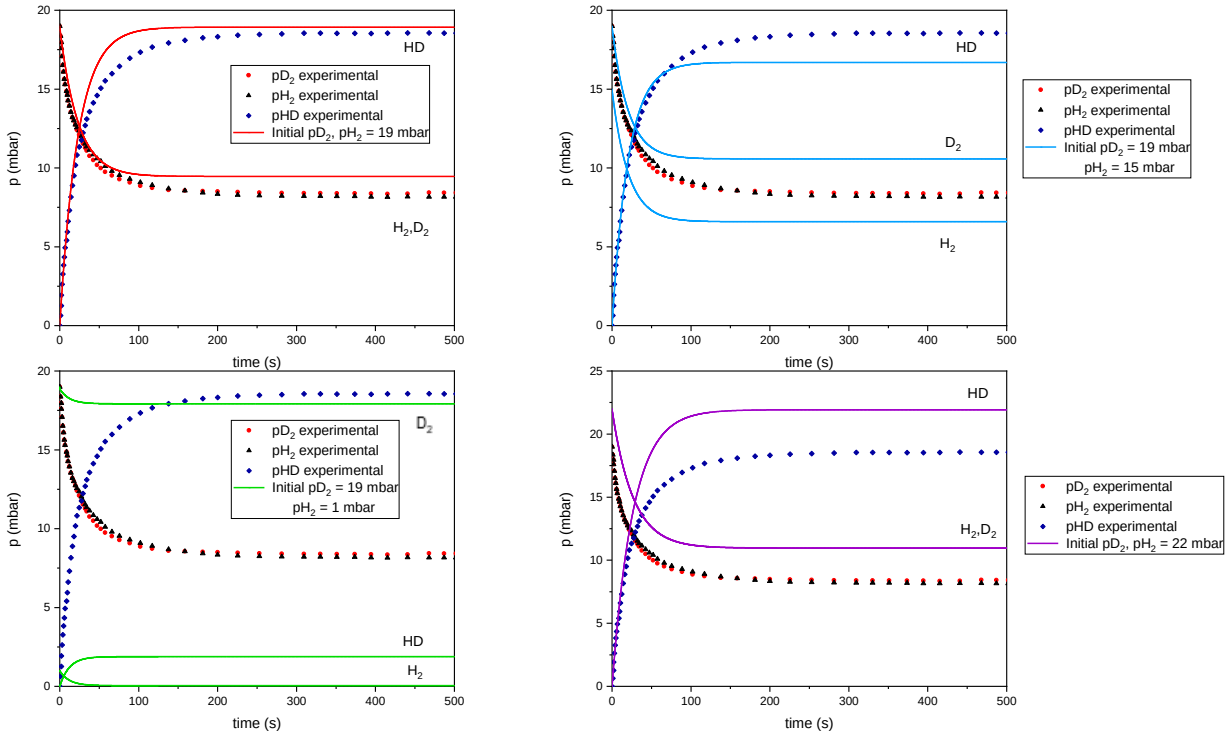

Figure 12. The influence of the initial partial pressure values of gases introduced into the reaction chamber on the partial pressure changes over time during the equilibration reaction.

The conversion percentage, along with the consumption of H_2 and D_2 individually, and as a sum, together with the amount of HD produced is available in Table 2.

The difference of conversion between these 4 cases lies in adsorption because during the calculations, right away the adsorption takes place at the very first moment in time. This means that a certain amount of H and D gets adsorbed on the metal sites immediately. This amount stays the same for all cases: $2.68 \cdot 10^{-5}$ mol·m^{-2}, this number shows the H and D surface concentration sum, but individually these values differ depending on the initial ratio of hydrogen and deuterium introduced into the reaction chamber.

For a) in Figure 12, the surface concentration of H and D is equal: $1.34 \cdot 10^{-5}$ mol·m^{-2} for each. For b), the surface concentration is different for these isotopes: cH = $1.1806 \cdot 10^{-5}$ mol·m^{-2}, cD = $1.496 \cdot 10^{-5}$ mol·m^{-2}. For c) scenario the difference between H and D surface concentration is the highest – cH = $1.338 \cdot 10^{-6}$ mol·m^{-2}, cD = $2.54 \cdot 10^{-5}$ mol·m^{-2}. In d) case it is the same as it was for a).

$$conversion = \frac{pHD_{produced}}{pH_{consumed} + pD_{consumed}} \cdot 100\% \quad (23)$$

The conversion percentages (see Equation (22)) are influenced by these values, not necessarily individual values of cH and cD, but possibly the sum of these values is the culprit. It has a significantly higher influence on c) in Figure 12 (also see Table 2), there is already a very low amount of hydrogen introduced to the reaction chamber (compared to the initial pD_2 value), so despite of there being plenty of deuterium, a relatively high amount of hydrogen gets adsorbed on the metal sites, never to be desorbed again (in calculations, that is). So, the conversion is quite a bit lower for this situation (93.1 %), whereas the difference is not very high for other examples that were analyzed (98.99 – 99.41 %).

Efficiency (see Equation (23)), on the other hand, depends on the ratio of initial H_2 and D_2 partial pressure. The higher the difference between these, the lower will be the efficiency, because for HD to form, both – hydrogen and deuterium – are needed. If one of them "runs out" in the process (graph c) would be an example of this), then HD production cannot progress if there are no other external sources. Another factor is the amount of hydrogen and deuterium initially, even if the ratio is 1:1. We see a higher efficiency for when 22 mbar (d) graph) for each (efficiency 99.68%), compared to 19 mbar (graph a)) for each where efficiency is slightly lower at 99.63%, this could be attributed to the overall higher pressure in the same volume of the reactor, we already understand the influence volume has on the system (see Figure 12).

$$efficiency = \frac{pHD_{produced}}{(pH_{2\ Initial} + pD_{2\ Initial})/2} \cdot 100\% \quad (24)$$

Including surface diffusion in such process can show how the partial pressure changes as some H species are provided from the support and can diffuse to the metal site to participate in the chemical reaction (see Figure 13). As it can be seen from the experimental results, the diffusion does not occur, the authors attribute it to the pretreatment procedure which ensures that no hydrogen is chemisorbed on the surface [34].

Table 2. Consumption, production, and conversion for Figure 12.

Graph	Initial partial pressure	Consumption	Production	Conversion	Efficiency
Experimental	H_2 = 19 mbar	H_2 = 10.83 mbar	HD = 18.56	86.77 %	97.68 %
	D_2 = 19 mbar	D_2 = 10.56 mbar			
	H_2+D_2 = 38 mbar	H_2+D_2 = 21.39 mbar			
a) red	H_2 = 19 mbar	H_2 = 9.53 mbar	HD = 18.93 mbar	99.32 %	99.63 %
	D_2 = 19 mbar	D_2 = 9.53 mbar			
	H_2+D_2 = 38 mbar	H_2+D_2 = 19.06 mbar			
b) blue	H_2 = 15 mbar	H_2 = 8.41 mbar	HD = 16.67 mbar	98.99 %	98.06 %
	D_2 = 19 mbar	D_2 = 8.43 mbar			
	H_2+D_2 = 34 mbar	H_2+D_2 = 16.84 mbar			
c) green	H_2 = 1 mbar	H_2 = 0.95 mbar	HD = 1.89 mbar	93.1 %	9.45 %
	D_2 = 19 mbar	D_2 = 1.08 mbar			
	H_2+D_2 = 20 mbar	H_2+D_2 = 2.03 mbar			
d) purple	H_2 = 22 mbar	H_2 = 11.03 mbar	HD = 21.93 mbar	99.41 %	99.68 %
	D_2 = 22 mbar	D_2 = 11.03 mbar			
	H_2+D_2 = 44 mbar	H_2+D_2 = 22.06 mbar			

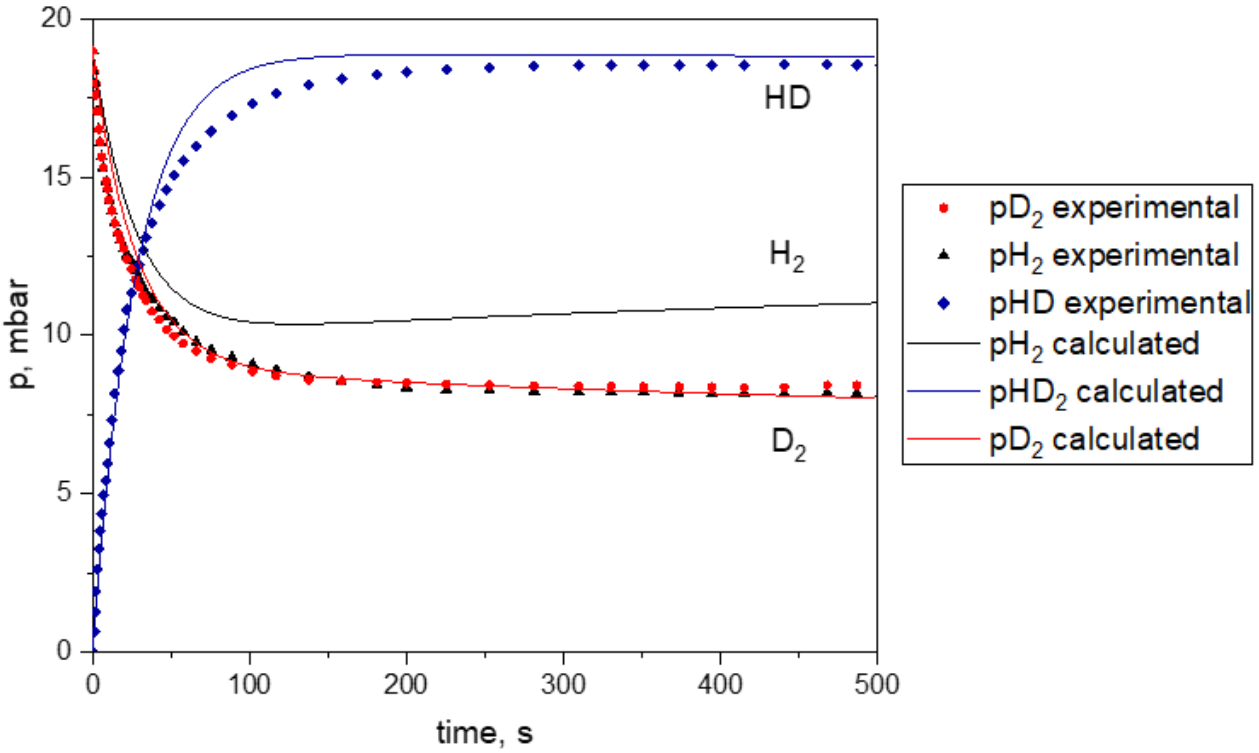

Figure 13. Experimentally [34] obtained curves of partial pressure of hydrogen (pH_2), deuterium (pD_2), and hydrogen product (pHD) over time during the isotopic hydrogen exchange on Ru/AC catalyst and the influence of including the surface diffusion process alongside the isotopic equilibration reaction theoretically estimated and reflected in terms of partial pressure over time. $D_s = 9 \cdot 10^{-19}$ $m^2 s^{-1}$.

If the surface diffusion were to theoretically occur, the expected change of the system could look as it does in Figure 13. It increases the consumption of D_2, as now it can travel from the metal site to the support and diffuse to its layers. The reverse happens to H_2 because when deuterium diffuses further from the metal site, this diffusion is compensated by the hydrogen that travels to the opposite direction. This means that as the time goes on, it appears that more H_2 begins to form because of this surface diffusion occurring.

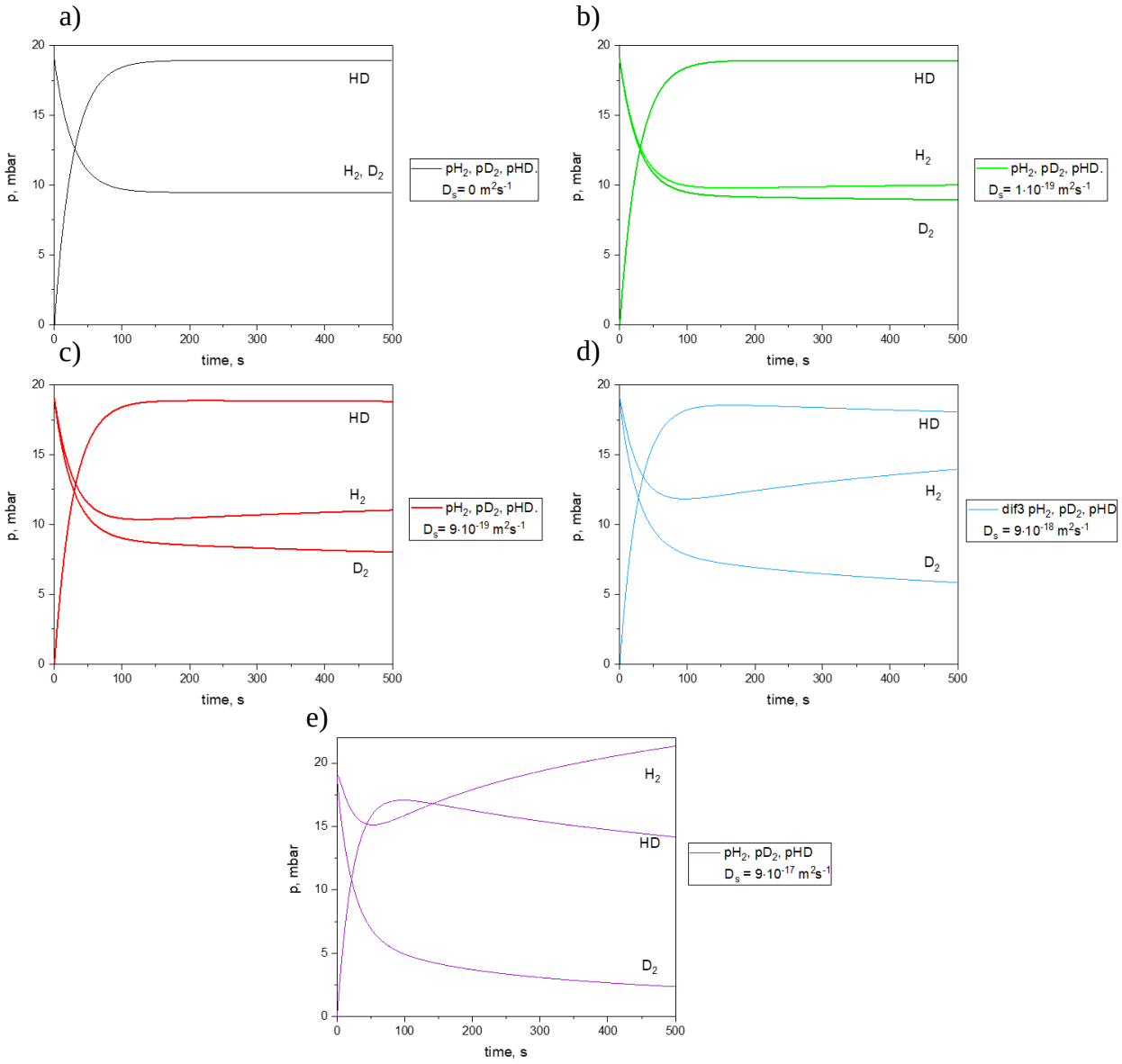

Figure 14. The influence of the surface diffusion process alongside the isotopic equilibration reaction reflected in terms of partial pressure over time with varying surface diffusion coefficients: a) $D_s = 0$, diffusion does not occur (black), b) $D_s = 1 \cdot 10^{-19}$ m^2s^{-1} (green), c) $D_s = 9 \cdot 10^{-19}$ m^2s^{-1} (red), d) $D_s = 9 \cdot 10^{-18}$ m^2s^{-1} (blue), e) $9 \cdot 10^{-17}$ m^2s^{-1} (purple).

In picture 14 we can see not only how the surface diffusion affects the system, but also to what extent does it influence the rate at which the steady state is achieved, if it affects the consumption of our two hydrogen isotopes H_2 and D_2, and the production of HD.

Diffusion does not occur in Figure 14 a), and we see the equal amount of both isotopes consumed during the reaction, reason being that the initial content of them was the same at 19 mbar.

When the surface diffusion exists, its coefficient determines how much of each isotope (H_2 or D_2) is consumed. The gap of partial pressure between hydrogen and deuterium increases as the diffusion coefficient increases, we see that significantly higher difference between the two appears in graph d) of Figure 14, compared to b) where its very sight, or a) where the gap is non-existent. In the blue graph we see that diffusion is so overpowering that it begins negatively affecting the HD production in the end stages of the experiment – the production begins decreasing, and H_2 begins to approach, and would possibly surpass, its initial value.

Table 3. Consumption, production, and conversion for Figure 14.

Graph, D_s	**Consumption**	**Production**	**Conversion**	**Efficiency**
a) black, $D_s = 0$ m^2s^{-1}	H_2 = 9.53 mbar	HD = 18.93 mbar	99.32 %	99.63 %
	D_2 = 9.53 mbar			
	H_2+D_2 = 19.06 mbar			
b) green, $D_s = 1\cdot10^{-19}$ m^2s^{-1}	H_2 = 9 mbar	HD = 18.92 mbar	99.27 %	99.58 %
	D_2 = 10.06 mbar			
	H_2+D_2 = 19.06 mbar			
c) red, $D_s = 9\cdot10^{-19}$ m^2s^{-1}	H_2 = 7.98 mbar	HD = 18.82 mbar	99.31 %	99.05 %
	D_2 = 10.97 mbar			
	H_2+D_2 = 18.95 mbar			
d) blue, $D_s = 9\cdot10^{-18}$ m^2s^{-1}	H_2 = 5.04 mbar	HD = 18.07 mbar	99.34 %	95.11 %
	D_2 = 13.15 mbar			
	H_2+D_2 = 18.19 mbar			
e) purple, $D_s = 9\cdot10^{-17}$ m^2s^{-1}	H_2 = -1.34 mbar	HD = 14.17 mbar	86.93 %	74.58 %
	D_2 = 17.64 mbar			
	H_2+D_2 = 16.3 mbar			

An interesting scenario occurs when the coefficient of surface diffusion is relatively high, at $9\cdot10^{-18}$ m^2s^{-1} as we see in graph e). The diffusion of deuterium from the metal site to the first, and other further layers of support is extremely fast. This flux of D is compensated by the flux of hydrogen to the opposite direction – towards the metal site. So much hydrogen travels outside of the far layers of the support to ruthenium and ends up in the gas phase that in the end the production of H_2 surpasses that of HD. A bizarre amount of deuterium is consumed in this case, and it does not result in a great HD production in this case, as the deuterium ever so quickly diffuses into the different layers of the support, a big chunk of it does not get a chance to react with hydrogen on the metal site to produce HD.

The trend for conversion percentage is not very straightforward, as is seen in Table 3. The higher the diffusion coefficient is, the less hydrogen and deuterium is used to produce HD. Some D goes to the support, so the overall consumption of D will always be higher for the cases where a higher coefficient of diffusion is used, however, the amount of H used for this purpose will be lower for higher D_s. When diffusion does not occur, the conversion rate is relatively high at 99.32 % where the support does not supply the system with H species. Then we see that when diffusion coefficient is increased,

it increases the overall conversion, up until the point where H production in the system surpasses that of HD, then the conversion is lower.

Efficiency, however, decreases with an increasing coefficient of diffusion. That is because the initially introduced H and D do not only participate in the production of HD as the main process, but a part of them end up moving in and out of the support, which ends up taking up some of the resources that could be used to produce HD but will not because they are further away from the metal site.

Unfortunately, this model was not able to correctly reflect the experiment where diffusion does occur in Ref. [34] (see Figure 15).

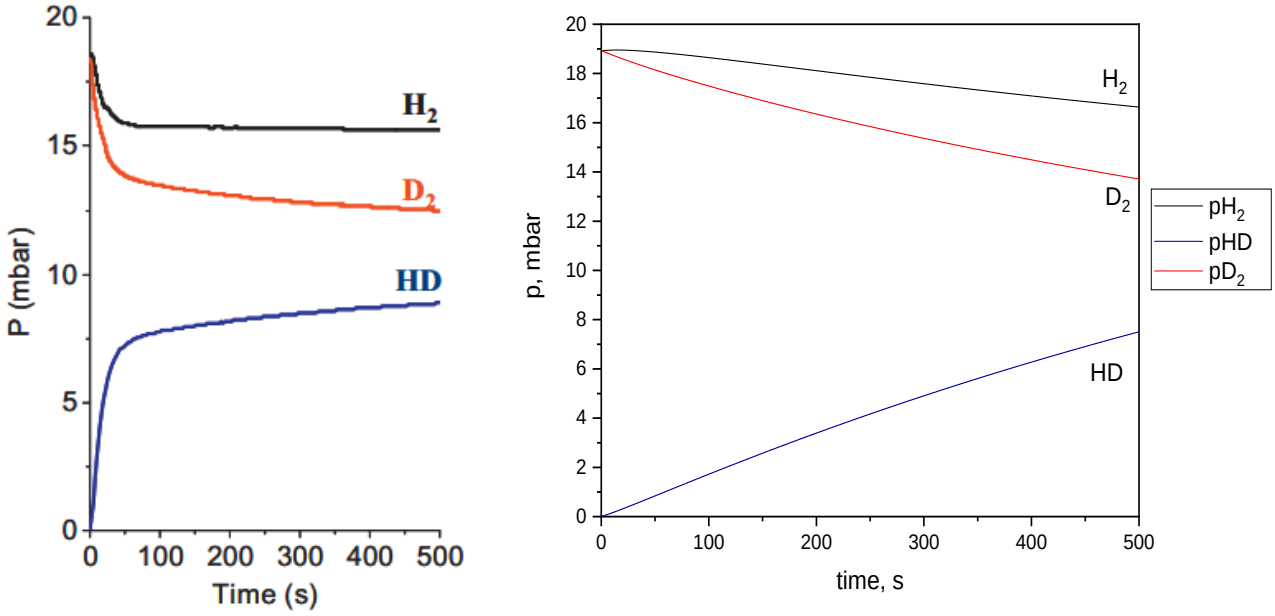

Figure 15. Partial pressure over time when surface diffusion takes place: during the experiment (left) [34], simulated using our kinetic model (right).

While the final values of partial pressure at 500s are in good agreement with the experimental values, the initial fast decrease of both H_2 and D_2 and the resulting fast production of HD in the first 50 s do not match the values calculated using our kinetic model. The reaction rate found during this attempt to fit the curves was 10500 m²/mol·s, and the diffusion coefficient was $9 \cdot 10^{-19}$ $m^2 s^{-1}$;

Further enhancements to the model would be necessary if one wishes to accurately describe this case of hydrogen isotopic exchange, however, these enhancements are beyond the scope of this work at present.

Even though there are differences between simulation and experiment, theoretically surface diffusion cannot be explained without the mention of surface concentrations of H and D on the metal site (first layer), as well as on the support (layers 2,3,4…). For this reason, these concentrations have been analyzed for Ru/AC catalyst. Diffusion coefficients were chosen to be the same as in Figure 13 to give a fuller view of the scenario that we already began analyzing. Figures 16-19 show surface concentrations for four cases: $D_s = 1 \cdot 10^{-19}$ $m^2 s^{-1}$, $D_s = 9 \cdot 10^{-19}$ $m^2 s^{-1}$, $D_s = 9 \cdot 10^{-18}$ $m^2 s^{-1}$, and $D_s = 9 \cdot 10^{-17}$ $m^2 s^{-1}$.

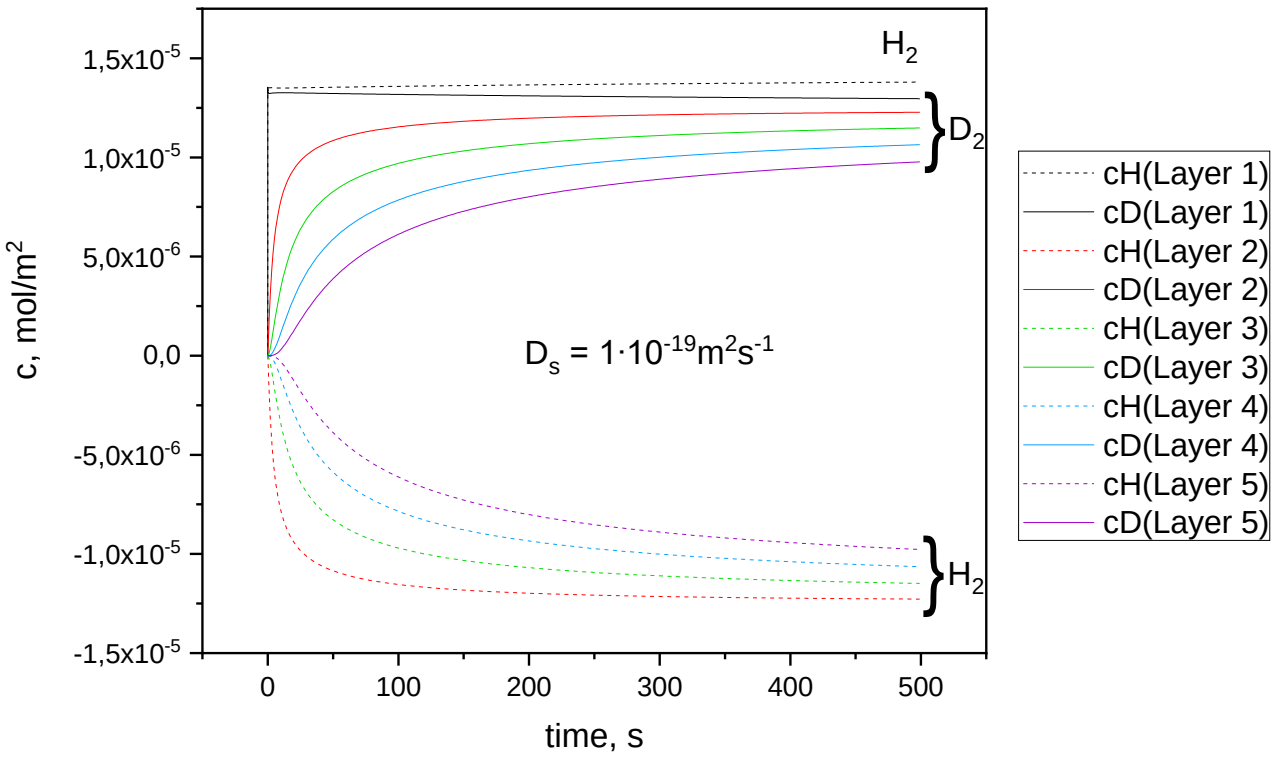

Figure 16. Surface concentration of hydrogen and deuterium for the first 5 layers over time during the isotopic hydrogen exchange and surface diffusion processes on Ru/AC catalyst, surface diffusion coefficient: $D_s = 1 \cdot 10^{-19}$ $m^2 s^{-1}$.

In Figure 16, in the first layer, the metal site (Layer 1), in the first moment in time (t = 0), the surface concentrations of H and D (cH and cD, respectively), are zero. First two moments in time will have cH and cD value of 0 for the second layer, three moments for the third layer, and so on. That is because this number of iterations is needed to even begin calculating these values in these layers. This is the case through Figures 16-19.

First layer in Figure 16 shows that cH and cD both, in the second moment in time, jump to $1.35 \cdot 10^{-5}$ $mol \cdot m^{-2}$, it is the adsorption which occurs instantly. From this point, cD slowly decreases over time as it diffuses from the metal site to the support. As much as cD decreases, the value of cH will increase, because their fluxes are the same, just in the opposite directions. The difference between cH and cD at the 500 s mark is $0.11 \cdot 10^{-5}$ $mol \cdot m^{-2}$ with cH(t=500) = $1.38 \cdot 10^{-5}$ $mol \cdot m^{-2}$ and cD(t=500) = $1.27 \cdot 10^{-5}$ $mol \cdot m^{-2}$.

In the second and further layers the behavior of cH and cD switches – cD increases, cH decreases and shows negative values. The minus sign shows that this much of cH leaves that layer as cD diffuses into it. This type of behavior will be present for all the graphs that represent cH and cD at layers higher than 1.

We see that in the first 100 seconds layers 2-5 begin filling up with deuterium quite fast. The second layer achieves the highest overall concentration, and does so the fastest, the opposite case being the

fifth layer, which is the case for all further layers, even though they are not presented in the graph. This is because some time needs to pass before these far-located layers will even be reached by deuterium. Later in time (for all the layers), the concentration values become more stable but slightly increasing.

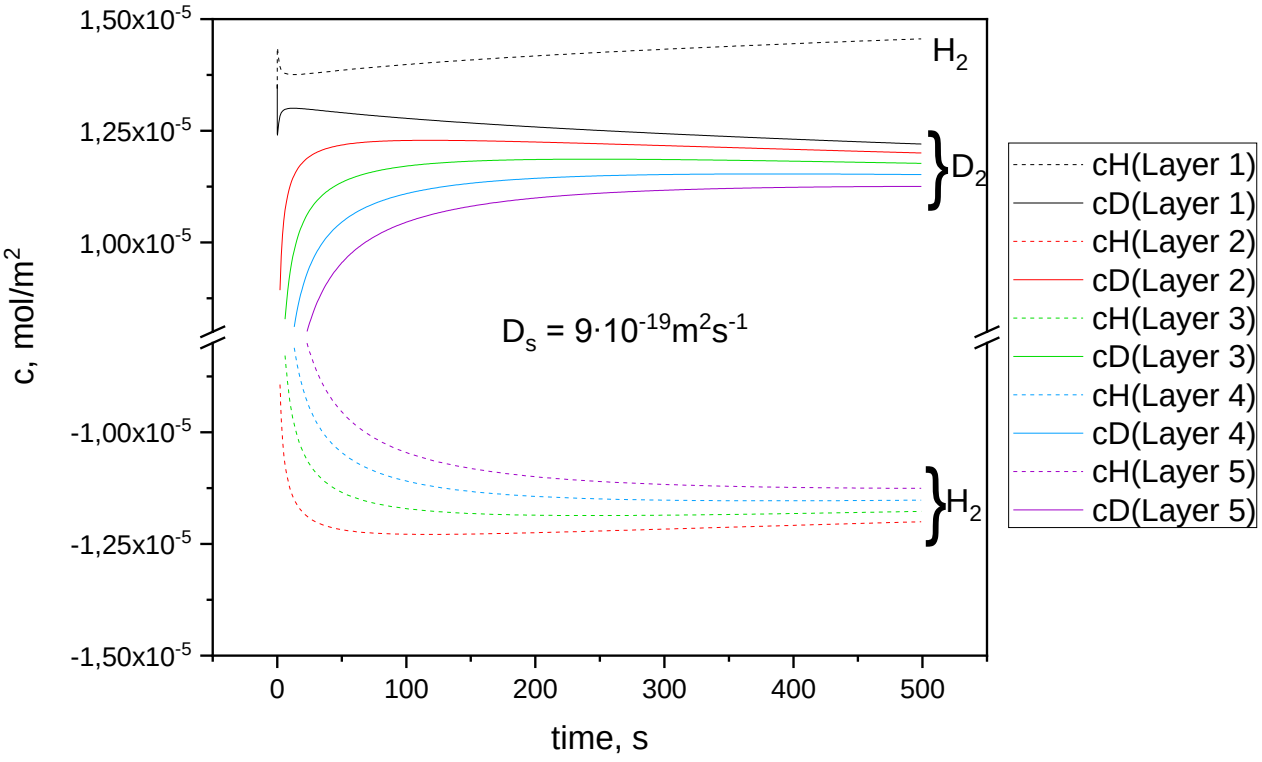

Figure 17. Surface concentration of hydrogen and deuterium for the first 5 layers over time during the isotopic hydrogen exchange and surface diffusion processes on Ru/AC catalyst, surface diffusion coefficient: $D_s = 9 \cdot 10^{-19}\ m^2 s^{-1}$.

Figure 17 shows the case where $D_s = 9 \cdot 10^{-19}\ m^2 s^{-1}$. Immediately, there is a noticeable change in the way surface concentrations behave in first layer. The difference between cH and cD at 500 s here is higher than in the previous case, being is $0.24 \cdot 10^{-5}\ mol \cdot m^{-2}$ with $cH(t=500) = 1.46 \cdot 10^{-5}\ mol \cdot m^{-2}$ and $cD(t=500) = 1.22 \cdot 10^{-5}\ mol \cdot m^{-2}$.

For layers 2-5 the increase of cD in the first 100 s is slightly higher for all the layers, it happens faster. After approximately 100 s we see the graphs forming a slight slope which shows cD decreasing ever so slightly towards the end. This decrease is very low because the diffusion coefficient is quite too low to cause a dramatic change here, however, we will see that this changes when diffusion coefficient is increased in graphs presented below.

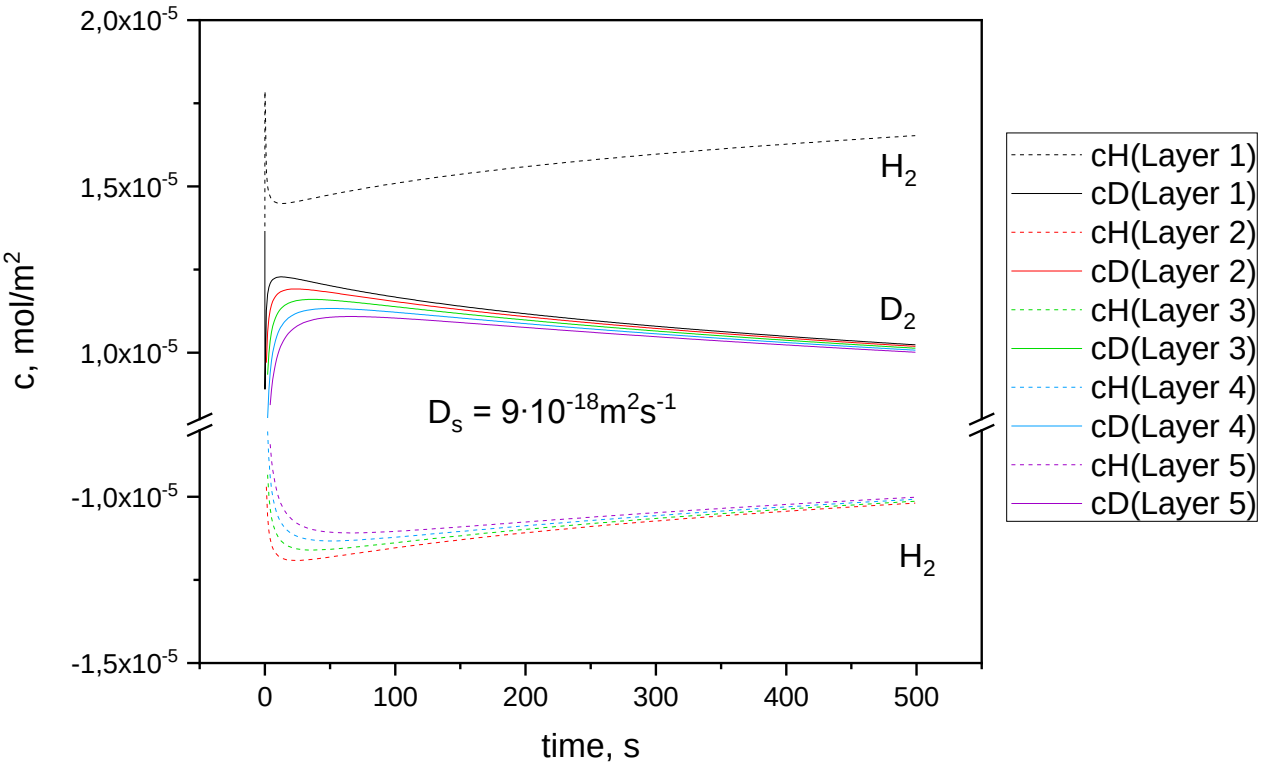

Figure 18. Surface concentration of hydrogen and deuterium for the first 5 layers over time during the isotopic hydrogen exchange and surface diffusion processes on Ru/AC catalyst, surface diffusion coefficient: $D_s = 9 \cdot 10^{-18}$ $m^2 s^{-1}$.

In Figure 18 surface concentrations are calculated for $D_s = 9 \cdot 10^{-18}$ $m^2 s^{-1}$. The difference between cH and cD in the first layer is even higher – $0.63 \cdot 10^{-5}$ $mol \cdot m^{-2}$ with cH(t=500) = $1.65 \cdot 10^{-5}$ $mol \cdot m^{-2}$ and cD(t=500) = $1.02 \cdot 10^{-5}$ $mol \cdot m^{-2}$.

The layers of the support are quickly filled with deuterium, the highest value for second layer is $1.19 \cdot 10^{-5}$ $mol \cdot m^{-2}$, which is slightly lower maximum value than for the previously analyzed case ($1.23 \cdot 10^{-5}$ $mol \cdot m^{-2}$) with a lower diffusion coefficient $D_s = 9 \cdot 10^{-19}$ $m^2 s^{-1}$. The flux is strong enough not to let D sit in the same layer for too long, forcing it to move forward – to further layers. The opposite occurs with cH values, to the same magnitude they increase over time.

The last example in Figure 19 shows that the difference between cH and cD in the first layer is the highest of all – $1.44 \cdot 10^{-5}$ $mol \cdot m^{-2}$ with cH(t=500) = $2.07 \cdot 10^{-5}$ $mol \cdot m^{-2}$ and cD(t=500) = $0.66 \cdot 10^{-5}$ $mol \cdot m^{-2}$. It shows that the higher the surface diffusion coefficient, the higher the difference between the surface concentrations values on the metal site at 500 s is. It only makes sense that the previously calculated conversion and efficiency percentages are the lowest for this case, because a wildly different amount of the isotopes is present on the metal site. This is not necessarily seen because of these specific values at 500 s, but the tendency throughout the time is clear – the cH and cD difference is maintained at the highest level for the highest diffusion coefficient.

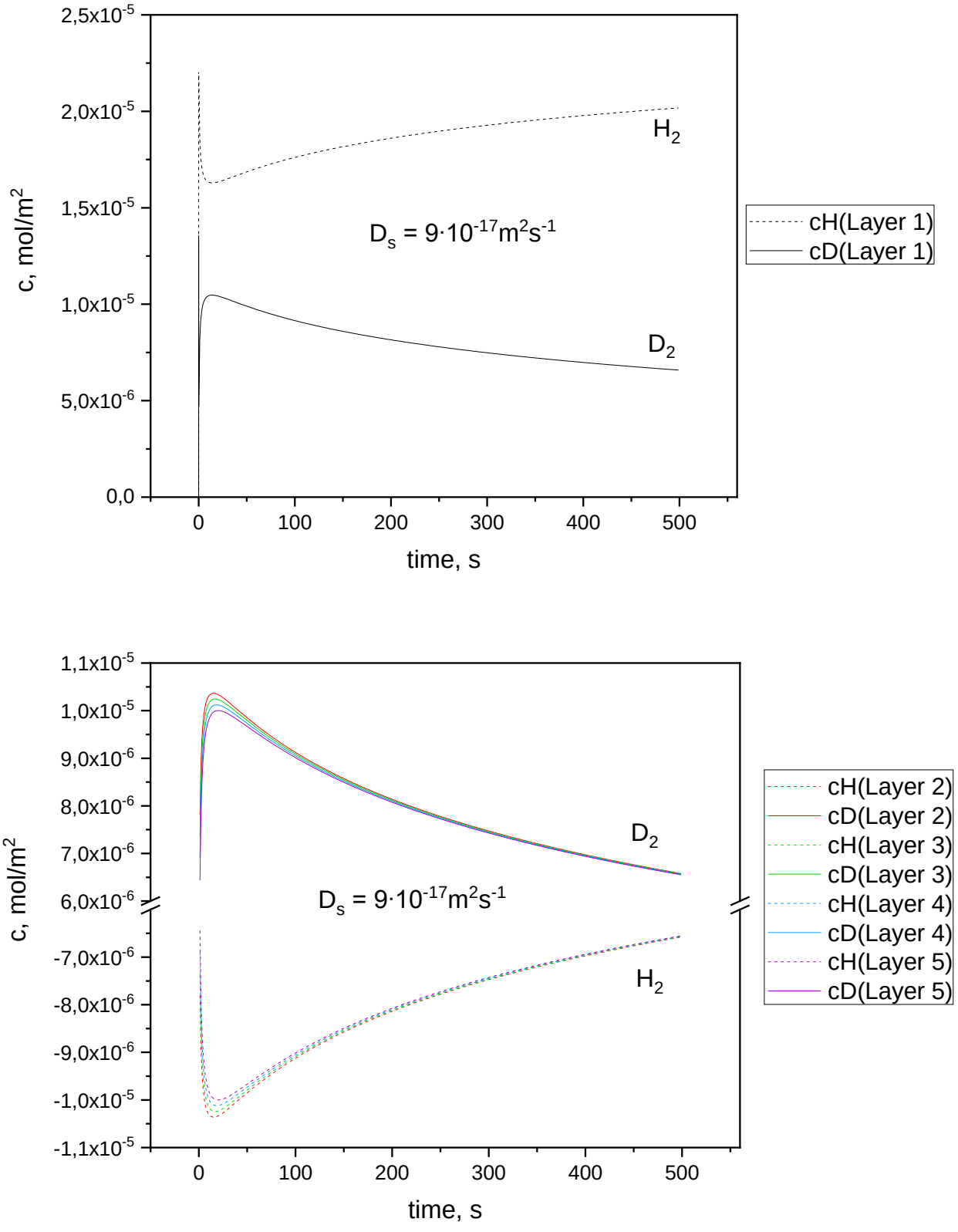

Figure 19. Surface concentration of hydrogen and deuterium for the first 5 layers over time during the isotopic hydrogen exchange and surface diffusion processes on Ru/AC catalyst, surface diffusion coefficient: $D_s = 9 \cdot 10^{-17}$ $m^2 s^{-1}$. First layer (top), layers 2-5 (bottom).

The scenario where two isotopes are initially introduced into the reaction chamber is not the only one possible. Fernández et al. [23] performed an experiment with a ruthenium-based catalyst with an aluminum oxide support. The experiment was also based on hydrogen isotopic exchange, but the strategy was to initially introduce only deuterium into the reaction chamber. This allows to see if any hydrogen is being provided by the support to the system. After tweaking some parameters, this experiment was also analyzed by our kinetic model (see parameters in Table 4).

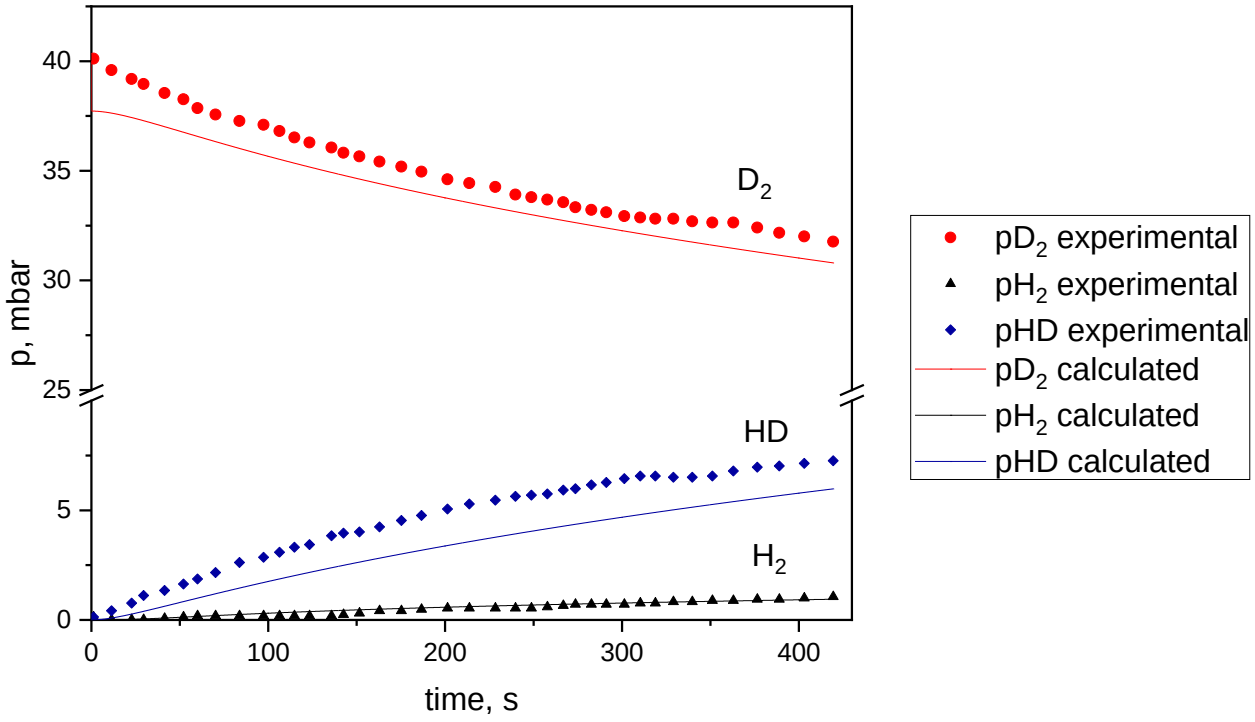

Figure 20. Experimentally [23] and theoretically obtained values of partial pressure of hydrogen (pH_2), deuterium (pD_2), and hydrogen product (pHD) over time during the isotopic hydrogen exchange and surface diffusion on the surface of Ru/Al_2O_3 catalyst.

Table 4. The parameters used in the kinetic model [23].

Parameter	**Value, units**
Volume of reactor (V) [23]	10 cm^3
Reaction rate (k)	1000 $m^2/mol \cdot s$
Weight fraction of Ru in the catalyst (f_{Ru}) [23]	1 %
Mass of the catalyst (m_{cat}) [23]	30 mg
Surface area of Ru (S_{Ru}) [23]	0.0345 m^2
Particle size of Ru (c_{Ru}) [23]	3.6 nm
Molar weight of Ru (M_{Ru})	101.07 g/mol
Diffusion coefficient (D_s)	$1.3 \cdot 10^{20}$ $m^2 s^{-1}$
Initial Partial Pressure of H_2 [23]	0 mbar
Initial Partial Pressure of D_2 [23]	40 mbar
Initial Partial Pressure of H_D [23]	0 mbar

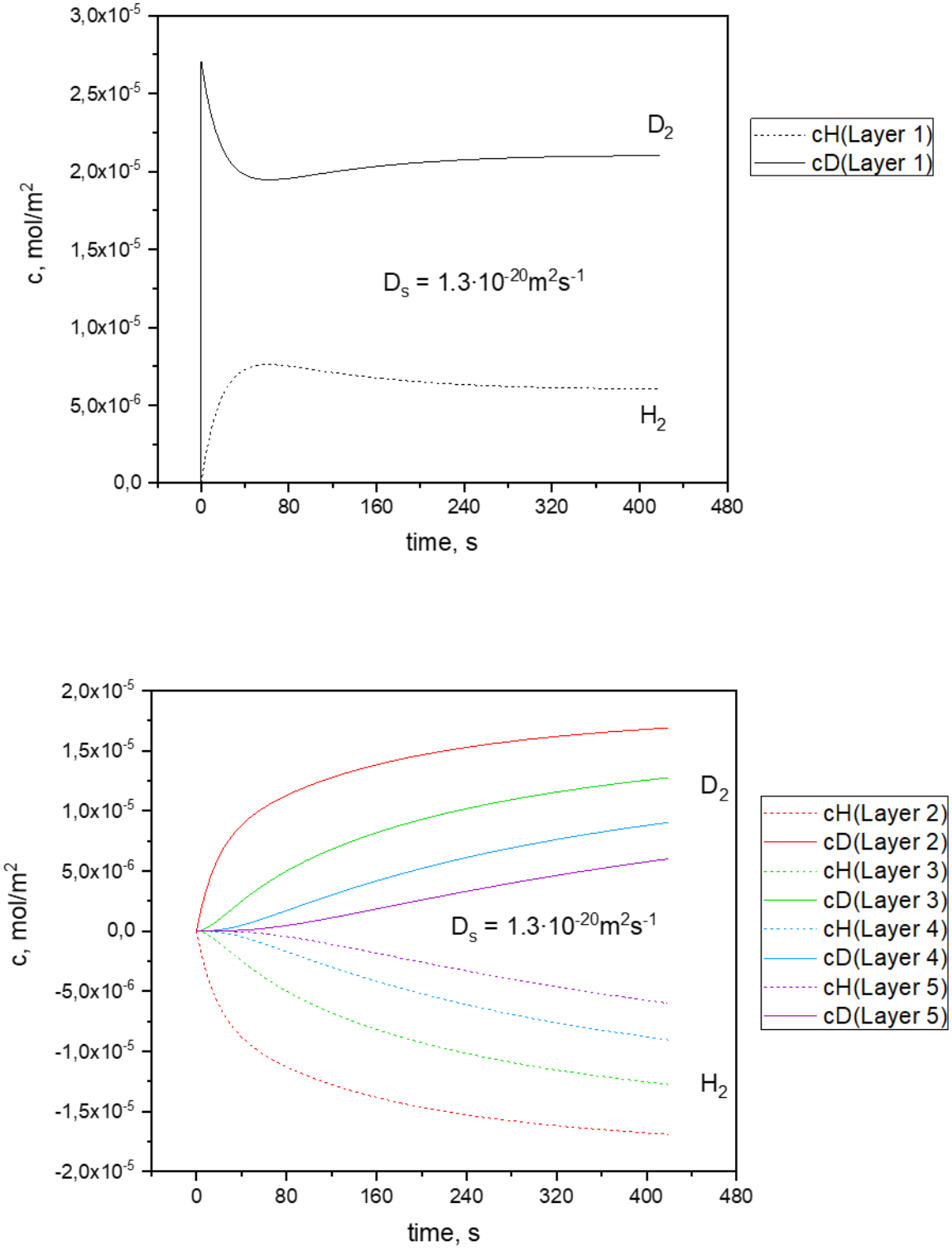

Figure 21. Surface concentration of hydrogen and deuterium for the first 5 layers over time during the isotopic hydrogen exchange and surface diffusion processes on Ru/Al_2O_3 catalyst, surface diffusion coefficient: $D_s = 1.3 \cdot 10^{-20}$ m^2s^{-1}. First layer (top), layers 2-5 (bottom).

The influence of diffusion on the surface layers is a little bit different in this case (Figure 21). That is because we initially start off with no external hydrogen source, it must come from the support. This time, in the first layer, cD starts off with a very high value in the second moment in time, while cH

slowly increases as cD is diffusing into deeper layers and cH flux travels to the opposite direction. A very high difference between cH and cD values is seen over time as well as in the last moments in time at 420 s ($1.5 \cdot 10^{-5}$ mol·m^{-2}). Paired with a very low diffusion coefficient, we get quite a low conversion (see Table 5).

Table 5. Consumption, production, and conversion for Figure 18.

Production	**Consumption**	**Conversion**
HD = 5.98 mbar	D_2 = 9.2 mbar	58.92 %
H_2 = 0.95 mbar		

Conclusions

1. Two experiments [34] (ruthenium catalyst on an activated carbon support: Ru/AC) and [23] (ruthenium catalyst on an aluminum oxide support: Ru/Al_2O_3) were referenced in this work, and the kinetic model was created for both. The initial parameters have been defined in the results section. In both experiments, adsorption, desorption, and chemical reactions occur. Surface diffusion has influence only on the second experiment.
2. Using "MATLAB" software, the occurring processes were described by kinetic equations in the form that is suitable to use when writing a code. Initial values, found in the two references of experiments, were used in the code along with the manually determined reaction rates: $k(Ru/AC) = 4.4 \cdot 10^5\ m^2 \cdot mol^{-1}s^{-1}$; $k(Ru/Al_2O_3) = 1000\ m^2 \cdot mol^{-1}s^{-1}$. Diffusion is only present in the experiment with Ru/Al_2O_3 catalyst, the coefficient of surface diffusion for this experiment was found to be $D_s = 1.3 \cdot 10^{-20}\ m^2s^{-1}$.
3. It was found that reactors volume and surface area of the noble metal impact the partial pressure over time in a way, that increasing the volume gives the same result as decreasing the surface area. Increasing the volume slows the process the same way as it would if the surface area of the metal was to be reduced. The partial pressure over time graph will be identical for the case when the volume is increased X times and for the case when the surface area is decreased X times. Dispersion was found to positively affect the hydrogen-deuterium (HD) production, as the higher value of dispersion is achieved when having smaller particles which results in the higher surface area of the metal, meaning that more metal is available for the reaction to take place on. This reflects in the results with using different percentages of dispersion: the reaction reaches a steady state faster with catalysts that have a higher level of noble metal dispersion. Mass and mass fraction of ruthenium are directly proportional to the surface area; therefore, these parameters affect the system in the same way that increasing the surface area would have – the reaction occurs faster.
4. The surface concentrations of hydrogen and deuterium on the metal site, when diffusion does not occur, will react a certain value in the first moments in time, and then remain constant throughout the time of the calculations. No hydrogen and no deuterium are present on the support if surface diffusion does not occur. In cases where diffusion plays a role and does so to varying degrees (different values of diffusion coefficients), not only the metal site but the support will have non-zero concentrations of H and D atoms. Diffusion coefficient influences the surface concentration on the entire catalyst. On the metal site (first layer) the concentrations of H and D differ during the entirety of the process, the gap between these values is the highest when the diffusion coefficient is the highest. Concentrations in the layers of support depend on the surface diffusion, too, the faster the diffusion, the faster the concentration of D reaches a high value, and then decreases faster, forming a relatively steep slope between the maximum value of the concentration reached in the first 100 s to the value at 500s. The changes in the support layers affect the concentration difference on the metal site, and it shows that the higher the difference of the concentration – the worse it is for the production of HD. $D_s = 0\ m^2s^{-1}$ efficiency is 99.63 % and decreases to 74.58% at $D_s = 9 \cdot 10^{-17}\ m^2s^{-1}$.
5. Using an equimolar mixture of H_2/D_2 initially, when diffusion does not occur, results in a higher amount of HD produced, compared to initially using only D_2 and having the support to supply the hydrogen atoms needed for the reaction to occur, especially if the surface diffusion coefficient is low in the second case.

List of references

1. Singh, Santosh. (2018). Enzyme Catalysis and Its Role in Food Processing Industries. 10.1007/978-981-13-1933-4_8.
2. Rahman R, Uahengo V, Likius D (2017) Green chemistry concept: Applications of catalysis in pharmaceutical industry. Glob Drugs Therap 2: DOI: 10.15761/GDT.1000130.
3. Lam, Y.L., Kan, C.W. and Yuen, C.W.M. (2012), "Application of Catalyst in Textile Wet Processes", Research Journal of Textile and Apparel, Vol. 16 No. 1, pp. 10-23.https://doi.org/10.1108/RJTA-16-01-2012-B002
4. Gao, Feng & Szanyi, Janos. (2020). Automotive Catalysis. 10.1002/9783527822508.ch73.
5. Kakaei, K., Esrafili, M. D., and Ehsani, A. (2019). Introduction to Catalysis. Graphene Surfaces - Particles and Catalysts, 1–21. DOI:10.1016/b978-0-12-814523-4.00001-0.
6. A. Kayode Coker, Coker A. Kayode, (2001). Modeling of Chemical Kinetics and Reactor Design, Gulf Professional Publishing. Pages xvii-xxx, ISBN 9780884154815. DOI: https://doi.org/10.1016/B978-088415481-5/50002-4.
7. Huazhang Liu, (2013). Ammonia Synthesis Catalysts Innovation and Practice. Chemical Industry Press, Beijing. ISBN 978-981-4355-77-3.
8. National Center for Biotechnology Information (2022). PubChem Compound Summary for CID 222, Ammonia. Retrieved April 16, 2022 from https://pubchem.ncbi.nlm.nih.gov/compound/Ammonia.
9. Seo, Youngkyun & Han, Seongjong. (2021). Economic Evaluation of an Ammonia-Fueled Ammonia Carrier Depending on Methods of Ammonia Fuel Storage. Energies. 14. 8326. 10.3390/en14248326.
10. Gezerman, Ahmet Ozan. (2022). A Critical Assessment of Green Ammonia Production and Ammonia Production Technologies. Kemija u industriji. 10.15255/KUI.2021.013.
11. Chai, W. S., Bao, Y., Jin, P., Tang, G., & Zhou, L. (2021). A review on ammonia, ammonia-hydrogen and ammonia-methane fuels. Renewable and Sustainable Energy Reviews, 147, 111254. doi:10.1016/j.rser.2021.111254.
12. Muhler, M. (1996). [Studies in Surface Science and Catalysis] 11th International Congress On Catalysis - 40th Anniversary, Proceedings of the 11th ICC Volume 101 || Ruthenium as catalyst for ammonia synthesis. 317–326. doi:10.1016/s0167-2991(96)80242-4
13. Tsyrul'nikov, P. G.; Iost, K. N.; Shitova, N. B.; Temerev, V. L. (2016). Methanation of the carbon supports of ruthenium ammonia synthesis catalysts: A review. Catalysis in Industry, 8(4), 341–347. doi:10.1134/s2070050416040115
14. Chen, Minxuan; Yuan, Mingwei; Li, Jinjun; You, Zhixiong (2018). Ammonia synthesis over Cs- or Ba-promoted ruthenium catalyst supported on strontium niobate. Applied Catalysis A: General, 554(), 1–9. doi:10.1016/j.apcata.2018.01.006
15. Rok Šivec, Matej Huš, Blaž Likozar, Miha Grilc, (2022). Furfural hydrogenation over Cu, Ni, Pd, Pt, Re, Rh and Ru catalysts: Ab initio modelling of adsorption, desorption and reaction micro-kinetics. Chemical Engineering Journal, Volume 436, 135070, ISSN 1385-8947. https://doi.org/10.1016/j.cej.2022.135070.
16. Lin, Bingyu; Guo, Yunjie; Lin, Jingdong; Ni, Jun; Lin, Jianxin; Jiang, Lilong; Wang, Yong (2017). Deactivation study of carbon-supported ruthenium catalyst with potassium promoter. Applied Catalysis A: General, 541(), 1–7. doi:10.1016/j.apcata.2017.04.020

17. Zbigniew Kowalczyk; Sławomir Jodzis; Wioletta Raróg; Jerzy Zieliński; Jerzy Pielaszek (1998). Effect of potassium and barium on the stability of a carbon-supported ruthenium catalyst for the synthesis of ammonia. , 173 (2), 153–160. doi: 10.1016 / s0926-860x (98) 00175-6
18. Ilenia Rossetti; Nicola Pernicone; Lucio Forni (2001). Promoters effect in Ru/C ammonia synthesis catalyst. , 208(1-2), 271–278. doi:10.1016/s0926-860x(00)00711-0
19. Huazhang Liu, (2014). Ammonia synthesis catalyst 100 years: Practice, enlightenment and challenge. Chinese Journal of Catalysis, Volume 35, Issue 10. Pages 1619-1640. ISSN 1872-2067. DOI: https://doi.org/10.1016/S1872-2067(14)60118-2.
20. Stacey E. Siporin, Robert J. Davis, (2004). Use of kinetic models to explore the role of base promoters on Ru/MgO ammonia synthesis catalysts, Journal of Catalysis, Volume 225, Issue 2, Pages 359-368, ISSN 0021-9517. https://doi.org/10.1016/j.jcat.2004.03.046.
21. Wang, Ziqing; Lin, Jianxin; Wang, Rong; Wei, Kemei (2013). Ammonia synthesis over ruthenium catalyst supported on perovskite type BaTiO3. Catalysis Communications, 32(), 11–14. doi:10.1016/j.catcom.2012.11.024
22. Magdalena Karolewska; Elżbieta Truszkiewicz; Bogusław Mierzwa; Leszek Kępiński; Wioletta Raróg-Pilecka (2012). Ammonia synthesis over cobalt catalysts doped with cerium and barium. Effect of the ceria loading. . 445-446 (none). -. doi: 10.1016 / j.apcata.2012.08.028
23. Fernández, Camila; Bion, Nicolas; Gaigneaux, Eric M.; Duprez, Daniel; Ruiz, Patricio (2016). Kinetics of hydrogen adsorption and mobility on Ru nanoparticles supported on alumina: Effects on the catalytic mechanism of ammonia synthesis. Journal of Catalysis, 344(), 16–28. doi:10.1016/j.jcat.2016.09.013
24. J. Polanski, 4.14 - Chemoinformatics, Editor(s): Steven D. Brown, Romá Tauler, Beata Walczak, (2009). Comprehensive Chemometrics, Elsevier. ISBN 9780444527011. https://doi.org/10.1016/B978-044452701-1.00006-5.
25. O. Lindblom, T. Ahlgren, K. Heinola, (2021). Molecular dynamics simulations of hydrogen isotope exchange in tungsten vacancies. Nuclear Materials and Energy, Volume 29, ISSN 2352-1791. DOI: https://doi.org/10.1016/j.nme.2021.101099.
26. Zengqi Lu, Jiamao Li, Xiaolong Fu, Jingwei Hou, Guangming Ran, Chengjian Xiao, Xiaolin Wang, (2022). Superhydrophobic Pt@SBA-15 catalyst for hydrogen water isotope exchange reactions, International Journal of Hydrogen Energy, Volume 47, Issue 41. Pages 18080-18087, ISSN 0360-3199. https://doi.org/10.1016/j.ijhydene.2022.03.279.
27. A. Galdikas. (2006). Matematinė medžiagotyra, ISBN 978-9955-686-22-4, KTU.
28. Andrew C. Turner, Nicholas J. Pester, Markus Bill, Mark E. Conrad, Kevin G. Knauss, Daniel A. Stolper, (2022). Experimental determination of hydrogen isotope exchange rates between methane and water under hydrothermal conditions. Geochimica et Cosmochimica Acta. ISSN 0016-7037, https://doi.org/10.1016/j.gca.2022.04.029.
29. Daiki Yamamoto, Noriyuki Kawasaki, Shogo Tachibana, Michiru Kamibayashi, Hisayoshi Yurimoto, (2021). An experimental study on oxygen isotope exchange reaction between CAI melt and low-pressure water vapor under simulated Solar nebular conditions, Geochimica et Cosmochimica Acta, Volume 314, Pages 108-120, ISSN 0016-7037. https://doi.org/10.1016/j.gca.2021.09.016.
30. Dominique Martin and Daniel Duprez, (1996). Mobility of Surface Species on Oxides. Isotopic Exchange of 18O2 with 16O of SiO2, Al2O3, ZrO2, MgO, CeO2, and CeO2-Al2O3. Activation by Noble Metals. Correlation with Oxide Basicity The Journal of Physical Chemistry 1996 100 (22), 9429-9438. DOI: 10.1021/jp9531568

31. Liang-Liang Zhao, Yixin Wu, Shiqing Huang, Zengyu Zhang, Wei Liu, Xiaoyu Yan, Ortho-Selective Hydrogen Isotope Exchange of Phenols and Benzyl Alcohols by Mesoionic Carbene-Iridium Catalyst, (2021). Organic Letters, Volume 23, Issue 23, Pages 9297-9302, ISSN 1523-7060. https://doi.org/10.1021/acs.orglett.1c03685.
32. Lijie Zhang, Xujun Liang, Quanying Wang, Yaoling Zhang, Xiangping Yin, Xia Lu, Eric M. Pierce, Baohua Gu, (2021). Isotope exchange between mercuric [Hg(II)] chloride and Hg(II) bound to minerals and thiolate ligands: Implications for enriched isotope tracer studies, Geochimica et Cosmochimica Acta, Volume 292, Pages 468-481, ISSN 0016-7037. https://doi.org/10.1016/j.gca.2020.10.013.
33. Amir Mosayebi, Mohammad Ali Mehrpouya, Reza Abedini, The development of new comprehensive kinetic modeling for Fischer–Tropsch synthesis process over Co-Ru/γ-Al2O3 nano-catalyst in a fixed-bed reactor, (2016). Chemical Engineering Journal, Volume 286, Pages 416-426, ISSN 1385-8947. https://doi.org/10.1016/j.cej.2015.10.087.
34. García-García, Francisco & Bion, Nicolas & Duprez, Daniel & Rodriguez-Ramos, I. & Ruiz, A.. (2015). H2/D2 isotopic exchange: A tool to characterize complex hydrogen interaction with carbon-supported ruthenium catalysts. Catalysis Today. 259. 10.1016/j.cattod.2015.03.014.
35. Galdikas, Arvaidas & Duprez, Daniel & Bion, Nicolas & Descorme, Claude. (2007). Oxygen Isotopic Exchange On Three-Way Catalysts: A Dynamic Kinetic Model. Materials Science. 13.
36. Galdikas, Arvaidas. (2004). A novel dynamic kinetic model of oxygen isotopic exchange on a supported metal catalyst. Applied Surface Science. 10.1016/j.apsus.2004.05.006.
37. Leterme, Charles; Fernández, Camila; Eloy, Pierre; Gaigneaux, Eric M.; Ruiz, Patricio (2017). The inhibitor role of NH 3 on its synthesis process at low temperature, over Ru catalytic nanoparticles. Catalysis Today, 286(), 85–100. doi:10.1016/j.cattod.2017.01.002
38. Epron, Florence (2020). Current Trends and Future Developments on (Bio-) Membranes || Hydrogen production by catalytic processes. 57–89. doi:10.1016/B978-0-12-817110-3.00003-5
39. Anderson, J. R., (1975). "Structure of Metallic Catalysts," Academic Press, New York. Available from: https://archive.org/details/structureofmetal0000ande.
40. Min Suk Choi;Hojin Jeong;Hyunjoo Lee, (2021). Re-dispersion of Pd-based bimetallic catalysts by hydrothermal treatment for CO oxidation . RSC Advances. doi:10.1039/d0ra09912k.